International
Progress Report

IPR-06-37

Äspö Hard Rock Laboratory

Canister Retrieval Test

Investigation of possible therminal induced stress damage by UCS testing and simulations

Sihai Luo

Jiangxi University of Science & Technology, P.R. China

December 2006

Svensk Kärnbränslehantering AB
Swedish Nuclear Fuel
and Waste Management Co
Box 5864
SE-102 40 Stockholm Sweden
Tel 08-459 84 00
+46 8 459 84 00
Fax 08-661 57 19
+46 8 661 57 19

Äspö Hard Rock
Laboratory

Report no.
IPR-06-37
Author
Sihai Luo
Checked by
Rolf Christiansson
Approved
Anders Sjöland

No.
F69K
Date
December 2006
Date
February 2007
Date
2007-03-07

Äspö Hard Rock Laboratory

Canister Retrieval Test

Investigation of possible therminal induced stress damage by UCS testing and simulations

Sihai Luo

Jiangxi University of Science & Technology, P.R. China

December 2006

Keywords: Canister Retrieval Test, Rock stress, DD0092G01, Micro fracturing, Uniaxial compression, Axisymmetric thermal analysis

Abstract

During the Canister Retrieval Test (CRT), the temperature around the deposition hole DD0092G01 was elevated and the stress in the rock was consequently increased. This report concerns the study to investigate if the increased stress around the deposition hole has led to micro fracturing in the surrounding rock and if the temperature and possible heat induced damage can be predicted by 2-Dimensional numerical simulation.

Uniaxial compression testing has been performed on 12 core samples taken from different parts of sub-horizontal core boreholes drilled parallel and perpendicular to the direction of the major principal stress in DD0092G01. The uniaxial compression strength (UCS) and Young´s modulus, the crack initiation stress (CIS) and crack damage stress (CDS), and the crack volumetric strain, have been compiled and analyzed. Comparisons were made according to the sampled direction and distance to deposition hole wall. Comparison was also made with results from testing on cores of the Äspö pillar stability experiment (APSE). It has been inferred, from the slightly higher values of crack volumetric strain at CIS, that some damage, but only to a small extent and in the form of micro fracturing, occurred in the rock near the deposition hole wall in the direction perpendicular to the major principal stress. There was no evidence of any damage from mechanical properties.

Axisymmetric thermal analysis and plane thermal-mechanical coupling analysis have been conducted by using FLAC2D. The temperature field from axisymmetric thermal analysis generally matches the measured results well, whereas the calculated temperature from plane analysis is much higher than measured. Much better results were obtained by applying the measured rock wall temperature as a temperature boundary. The numeric modelling results using this heat boundary condition show that, at depth 3.1m and 5.4m, in the rock near the deposition hole wall in the direction perpendicular to the major principal stress, the tangential stresses were higher than CIS after excavation, and at all three depths in the mentioned rock, the calculated tangential stresses at the temperature peak were higher than corresponding CIS and even near to CDS for depth 3.1m and 5.4m. Sensitivity analysis shows the main uncertainties regarding the modelling did not change this relationship. It seems from the numerical simulation that obvious stress induced damage should have occurred in the corresponding part of the rock volume.

The discrepancy in the degree of damage between the result from UCS testing and that from numerical simulation possibly indicates that the influence of the swelling pressure of the bentonite has a potential to reduce the stress induced damage of the rock.

Sammanfattning

Under Återtagsförsöket ökade temperaturen i berget runt deponeringshål DD0092G01, och som en följd av detta ökade även bergspänningarna. Denna rapport redovisar resultaten av en studie av i vad mån dessa termiskt inducerade spänningar kan ha förorsakat mikrosprickbildning i berget. Denna process har studerats med hjälp av 2-D numerisk simulering.

Enaxligt tryckförsök har genomförts på 12 st borrkärnor som tagits ut i horisontella borrhål från DD092G01, parallellt och vinkelrätt mot största huvudspänningen. Enaxlig tryckhållfasthet, E-modul, crack initiation stress, crack damage stress samt volymetrisk töjning har sammanställts och analyserats. Jämförelser mellan olika provtagningsriktningar, samt avstånd från deponeringshålets vägg har gjorts. Jämförelser gjordes även mot resultat från motsvarande tester av prover från Pelarstabilitetsförsöket (APSE). Det är indikerat av en liten ökning i volymetrisk töjning i form av mikrosprickor nära deponeringshålets yta i riktningen vinkelrätt mot största huvudspännngen.. Det finns inga tydliga belägg från de mekaniska lab-resultaten på skador i berget.

Axisymetrisk termisk analys och termo-mekanisk analys har utförts med FLAC2D. Analys av värmespridning i den axisymetriska analysen överensstämmer tämligen väl med mätdata, medan plain strain analys beräknar en högre temperatur än uppmätt. Bättre överensstämmelse i temperaturutveckling i berget erhölls när den mätta temperaturutvecklingen på deponeringshålets yta ansattes som randvillkor. De numeriska resultaten påvisar för de studerade djupen (3,1 och 5,4 m) att berget nära konturen i en riktning vinkelrätt mot största horisontalspänningen påvisar en tangentialspänning högre än crack initiation stress när hålets borrats. Simulering av tillståndet då maximal temperatur uppnåtts visar en tangentialspänning högre än crack initiation stress, och till och med nära crack damage stress på 3,1 0ch 5,4 m djup. Känslighetsanalyser visar att modellosäkerheter inte påverkar resultaten nämnvärt. Det bedöms därför från de numeriska resultaten som troligt att spänningsinducerad sprickbildning skulle kunna uppstå i delar av bergvolymen.

Skillnaden i resultat mellan analys av resultat från enaxlig provning och numerisk simulering indikerar att det utvecklade svälltrycket från bentoniten har en positiv effekt att begränsa spänningsinducerat brott i berget nära deponeringshålet.

Contents

1 Introduction

1.1 Background

The Canister Retrieval Test (CRT) was a test of a full size copy of a repository with a deposition hole (DD0092G01) heated and mainly aimed to test methods for canister retrieval from a saturated buffer. During the period from October 2000 to November 2005, the canister in the hole was heated with a maximum heat power of 2600W. Therefore, the surrounding rock of the hole was heated and the temperature was elevated.

A temperature increase in a rock volume with fixed boundaries leads to temperature induced strain which increases the stresses in the rock volume. Therefore, there was the concern for the CRT rock volume that if the increased stress around the deposition hole has led to micro fracturing in or any other damage to the surrounding rock and how to estimate and evaluate its occurrence.

The temperature and stress changes in the rock, and the temperature, relative humidity, pore pressure and total pressure in the buffer during the heating stage were measured.

1.2 Objectives

The objectives of this study were:

1. to investigate if the increased stress around the deposition hole has lead to micro fracturing or any other damage in the surrounding rock;
2. to test the capability of 2D numerical simulation to predict the heat induced temperature, stress and damage in the surrounding rock around such a heated deposition hole.

1.3 Methodologies

For this study, uniaxial compressive testing and the commercial Code FLAC2D (5.00) were used.

Uniaxial compressive tests were conducted on core samples taken from different parts of the sub-horizontal core boreholes drilled in DD0092G01 both parallel and perpendicular to the direction of the major principal stress. Comparisons of testing results were made among samples taken from different directions and different distance to the deposition hole wall. Comparison was also made with results from testing on cores of the APSE. The micro fracturing or damage was mainly examined and identified by crack-related parameters, with the focus on crack volumetric strain during the elastic stage of uniaxial compressive tests.

FLAC2D (5.00) was used to model the excavation and the heating process of the deposition hole. Temperature in the rock was calculated by treating the case either as a horizontal two dimensional or a vertical axisymmetric problem and obtained results were compared with the measured results, whereas stress was calculated from horizontal two dimensional thermal-mechanical coupling analysis and calculated results were applied to damage analysis.

Results from UCS testing and from numerical simulation were compared and discussed.

2 Geological background

The tunnel for the canister retrieval test is a part of the TASD-tunnel and situated approximately on the 420m-depth of the tunnel system at the Äspö Hard Rock Laboratory. The total length of TASD is 100m, of which the Canister Retrieval Test Tunnel (CRT-tunnel) constitutes the inner 20m (approximately section 84.0-100.5). To accommodate the canisters, two large deposition holes (DD0086G01 and DD0092G01), with the central spacing of 6m and the diameter of 1.75m, were drilled to the approximate depth of 8.5m by specially made vertically drilling Robbins TBM in 1999. Only DD0092G01 was used for CRT, the other hole (DD0086G01) was used for TBT (Temperature Buffer Test) later. See Figure 2-1 for the locations of the holes.

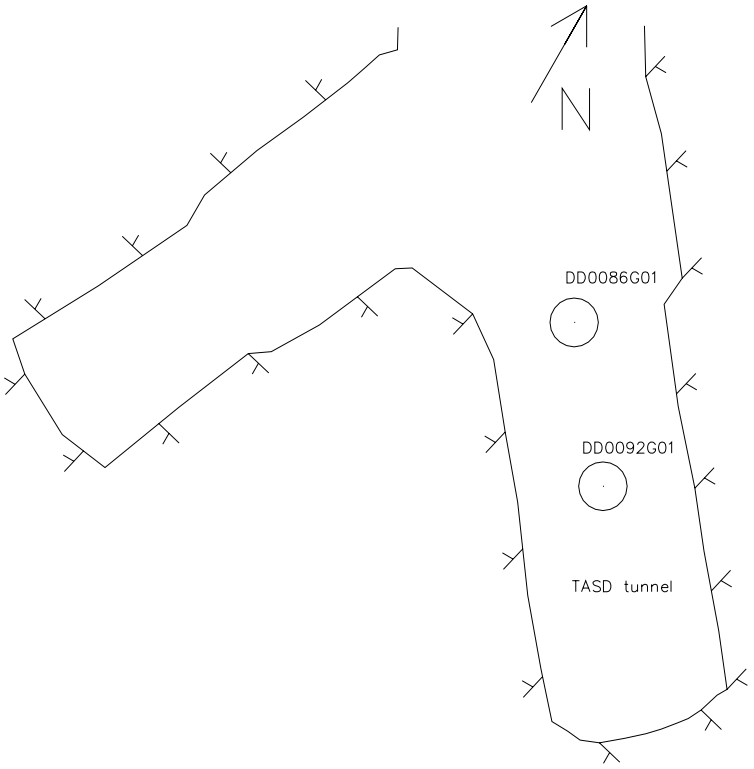

Figure 2-1. *The Location of Deposition holes.*

2.1 Rock type

Four rock types are present in the Canister Retrieval Test Tunnel and the deposition holes. The dominating rock type in the Canister Retrieval Test Tunnel is greenstone (56%). The second most common type is Äspö diorite (31%). Fine-grained granite is the third most common rock type (11%) and pegmatite is the least occurring type (2%).

The same four major rock types, Äspö diorite, greenstone, fine-grained granite, and pegmatite, have been distinguished in DD0092G01. Äspö diorite is mainly of the feldspar megacryst bearing type and it is partly slightly schistose. It constitutes about 30% of the hole-surfaces (wall and bottom) and appears mainly in the lower half of the hole. Greenstone is medium-grained and constitutes 38% of the hole and mainly occurs at upper half of the hole. Fine-grained granite constitutes 25% of the hole-surfaces. Pegmatite constitutes only about 5% of the surfaces.

The rock has been regarded as fresh (no alteration), besides some minor oxidation of the rock commonly in connection with fractures. The contacts between the rock types are mostly tight and sharp. More diffuse contacts are commonly found where a distinct rock type grades into a hybrid one.

2.2 Fractures

Four fracture sets are present. One of the sets is composed of fractures that are gently – steeply dipping mostly towards the S - SW and striking W-NW. Two rather steeply dipping sets are E-ESE dipping and N-NNE striking and NE-ENE dipping and NNW-NW striking, respectively. In the deposition hole, it is evident that sub-horizontal fractures are represented as well.

Most fractures contain more than one type of filling. Chlorite is by far the most common fracture filling and is found in 65-80% of all fractures. The fracture surfaces are mostly planar and rough. Most of the fractures (about 90%) in the tunnel floor as well as in the deposition holes are shorter than 2m and more than 50% of the fractures are less than 1m in length (cut-off 0.5m). 65-75% of the fractures in the deposition hole were healed and tight. Induced/natural open fractures (formerly healed and tight fractures that have been mechanically reopened) constitute most of the remaining fractures.

Water in minor quantities was found only at a few locations, of which some were patches on the rock surface and some were fractures. The water-bearing fractures in the deposition holes are mostly E-W to WNW striking and gently to steeply dipping, where as those in the tunnel are almost N-S striking and steeply dipping. In the deposition hole DD0092G01, six of the observed seven locations of water leakage appeared in the upper 3m of the hole. Seepage as drops and wet surface below, all the way down to the bottom of the hole, has been found to originate from 0.2x0.2m patches in the rock mass itself. Water inflow into the hole is approximately 5.1 litres per 24 hours. As a whole, the Canister Retrieval Test Tunnel must be regarded as a very dry part of the Äspö tunnel system.

The RMR-values (approximately 65-80) indicate that the rock mass of the Canister Retrieval Test Tunnel and the deposition holes is the same good quality as most parts of the HRL.

3 Experiment description

3.1 Experiment set-up

The deposition hole (DD0092G01) for CRT is located in TASQ at the depth of about -420m and has a diameter of 1.75m and depth of 8.5m. The other deposition hole (DD0086G01), with the same size and spaced 6m away, originally for the same purpose, was not used for CRT but used as TBT and was heated about 880days later.

In CRT, the test installation mainly consisted of a full-scale deposition hole as previously described, a copper canister equipped with electrical heaters and bentonite blocks (cylindrical and ring shaped). A 0.15 meter high concrete foundation was built at the bottom of the deposition hole. A copper canister of the full size, obtained from SKB's Encapsulation Project, with heaters inside it, was placed inside the hole. The canister is 1,050 mm in diameter, 4.83 m in height and has the weight of 21.4 tonnes. The bentonite buffer was installed in the form of blocks and rings, with an initial density of 1,710 and 1,790 kg/m^3, respectively and initial water content of 17%. The blocks have a diameter of 1.65 m and a height of 0.5 m. When the stack of blocks was 6 m high, the canister, equipped with electrical heaters, was lowered down in the centre of the hole and the cables to the heaters and instruments were connected. Additional blocks were emplaced until the hole was filled to a distance of one meter from the tunnel floor. The top of the hole was sealed with a retaining plug made of concrete and a steel plate. The plug was secured against heave caused by the swelling clay with nine cables anchored in the rock. Strips of matting were attached to the rock wall. Water was supplied artificially for saturation around the bentonite blocks. The cables from all instrumentation in the bentonite, deposition hole wall, canister, and from heaters in the canister, and the pipes for water supply, were placed in four types of slots cut in the hole wall (100–200mm wide, 40–60mm deep and 2200 or 3100mm long). Between the bentonite rings and blocks and the rock surface, the gap was filled with bentonite pellets and water. The average dry density of a single pellet was 1,800 kg/m^3, but the average dry density including voids after filling was estimated to be 1,130 kg/m^3 according to tests performed before the field installation. The natural initial water ratio of the pellets was 10%, and after the voids were filled with water the average water ratio was about 45%.

The TBT set-up is similar to that of CRT, but with a different heating system: two canisters (3 m long, 0.6 m in diameter) with maximum total heat power of 3000W.

The experimental set-up is shown in Figure 3-1(a), (b).

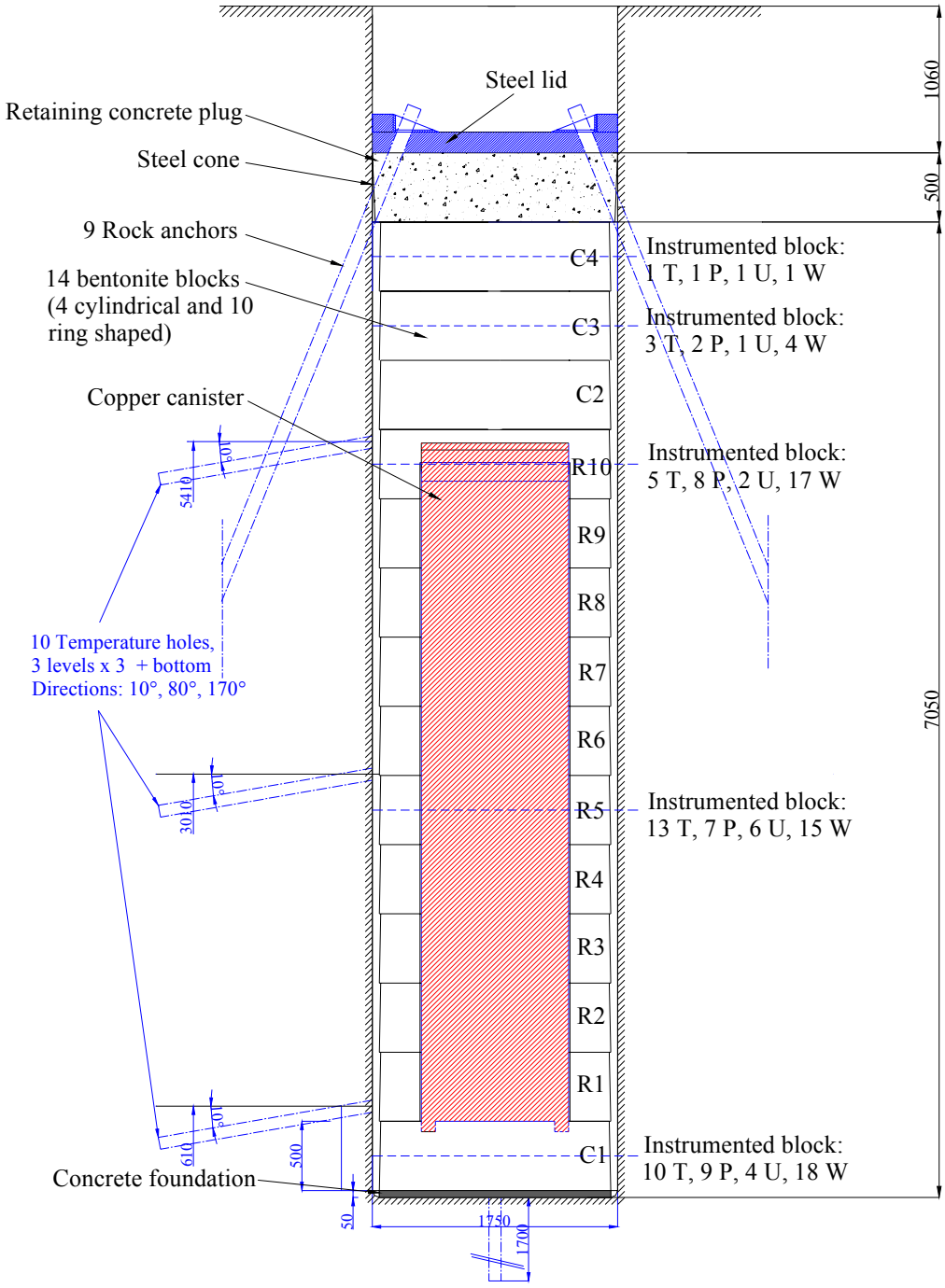
Steel lid
Retaining concrete plug
Steel cone
9 Rock anchors
14 bentonite blocks
(4 cylindrical and 10
ring shaped)
Copper canister
10 Temperature holes,
3 levels x 3 + bottom
Directions: 10°, 80°, 170°
Concrete foundation
C4
C3
C2
R10
R9
R8
R7
R6
R5
R4
R3
R2
R1
C1
Instrumented block:
1 T, 1 P, 1 U, 1 W
Instrumented block:
3 T, 2 P, 1 U, 4 W
Instrumented block:
5 T, 8 P, 2 U, 17 W
Instrumented block:
13 T, 7 P, 6 U, 15 W
Instrumented block:
10 T, 9 P, 4 U, 18 W
1060
500
7050
80
5410
80
3010
80
610
500
50
1750
1700

(a) CRT

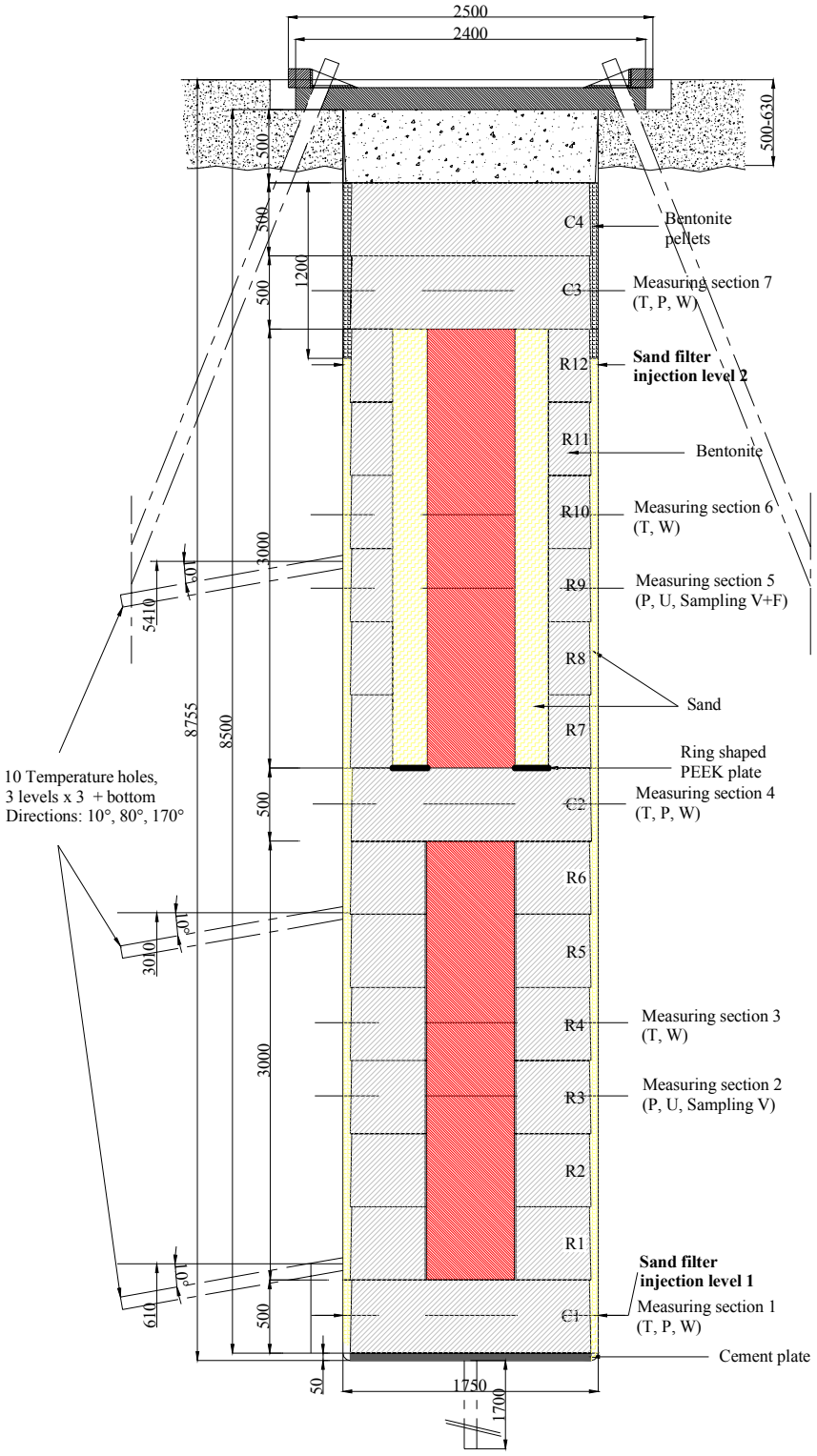

(b) TBT

Figure 3-1. *Sketch of Experiment Set-up.*

3.2 Measurements in the buffer and rock

The thermal, hydraulic and mechanical processes in the bentonite were measured during the whole heating stage by 128 installed instruments, including measurements of temperature at 32 points, total pressure at 27 points, pore water pressure at 14 points and relative humidity at 55 points. The locations corresponding to the top, the middle and the bottom of the canister were of most interest and densely instrumented. The instruments for radial measurements were mostly located at 585, 685 and 785mm from the center of the hole.

Measurements in the rock during the test included stress change and temperature monitoring. The stress monitoring included measurements of stress changes around the deposition hole in four cored boreholes parallel to the deposition hole. The installation holes (diameter 60 mm) were drilled 0.3m from the periphery of the deposition hole at four perpendicular locations, as shown in Figure3-2. The depth of A1,D1 B2,C2 was about 4m, B1, C1 about 7m and A2,D2 about 1.5m.

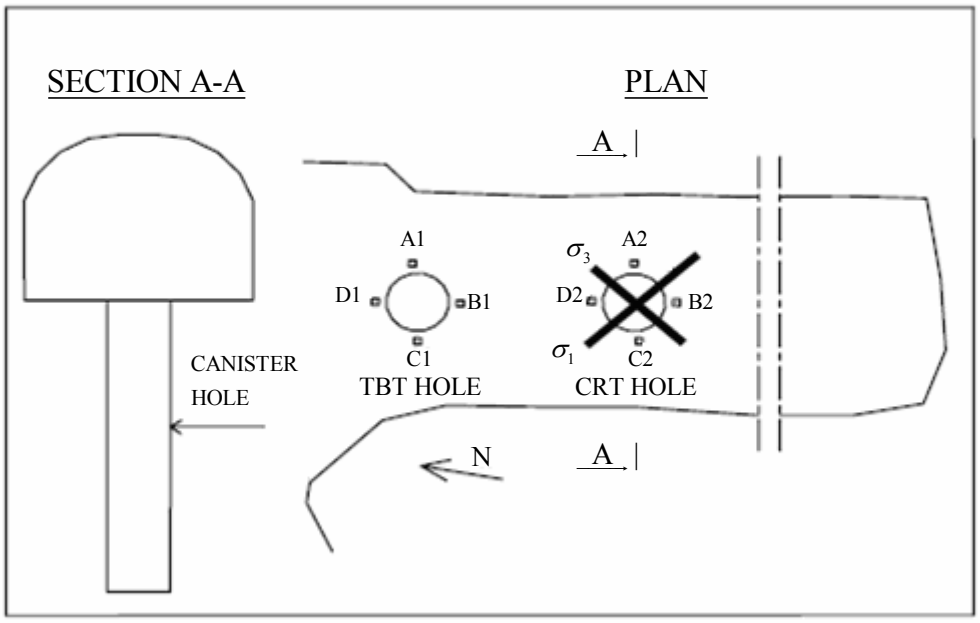

Figure 3-2. *Stress measurement layout.*

The temperature monitoring included measurements of temperatures radially from the deposition hole and from bottom. Radial measurements were monitored in three directions (near N, E and N160^{0}E) at three depths (3.1m, 5.5m and 7.9m from the leveled tunnel floor) on the hole wall. The holes drilled in the periphery of the deposition hole were inclined 10° in order to ensure that the thermocouples were perfectly embedded in the grout material. The thermocouples installed in each hole were at the distance of 0, 0.375, 0.75 and 1.50m from the deposition hole surface.

3.3 Heating process

The heating of the CRT canister started with an initially applied constant power of 700 W on October 27, 2000, raised to 1700 W on November 13(day 17) and further to 2600 W on February 13, 2001 (day 103), reduced to 2100 W on day 683 (September 10, 2002) and to 1600 W on day 1135 (December 4, 2003) and further to about 1150 W on day 1596 (March 10, 2005). No power was generated during one day between November 5 and 6, 2001 (day 375) and one week between March 4 and 11 2002 (days 495 to 502). On October 11 (day 1811) the power was switched off in order to prepare for the dismantling, excavation and retrieval of the test, which were carried out in the beginning of 2006. On March 26, 2003 (day 881), heating of TBT in deposition hole ((DD0086G01) started, and its maximum power is 2X1500W. The heating is still ongoing.

The variation of the power with time (days from October 27, 2000) can be seen from Figure 3-3.

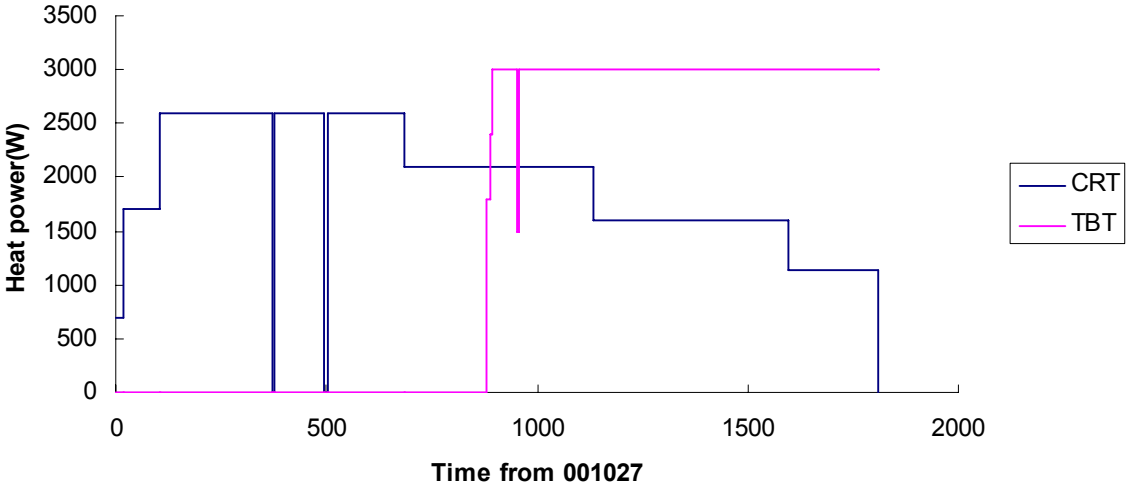

Figure 3-3. *The heat power in CRT and TBT.*

3.4 Process in the buffer

The bentonite pellets and water were filled into the gap between the rock surface and bentonite blocks on October 26, 2000 and the heating of the canister started one day later. As a result, the temperature and the saturation degree in the bentonite blocks began to increase and the bentonite began swelling, which consequently increased the total pressure (summation of pore water and swelling pressure). Figure3-4 through Figure3-6 are measured results of temperature, relative humidity and total pressure obtained from bentonite ring 5 (about 5.5m deep from the tunnel floor and near the middle height of the canister).

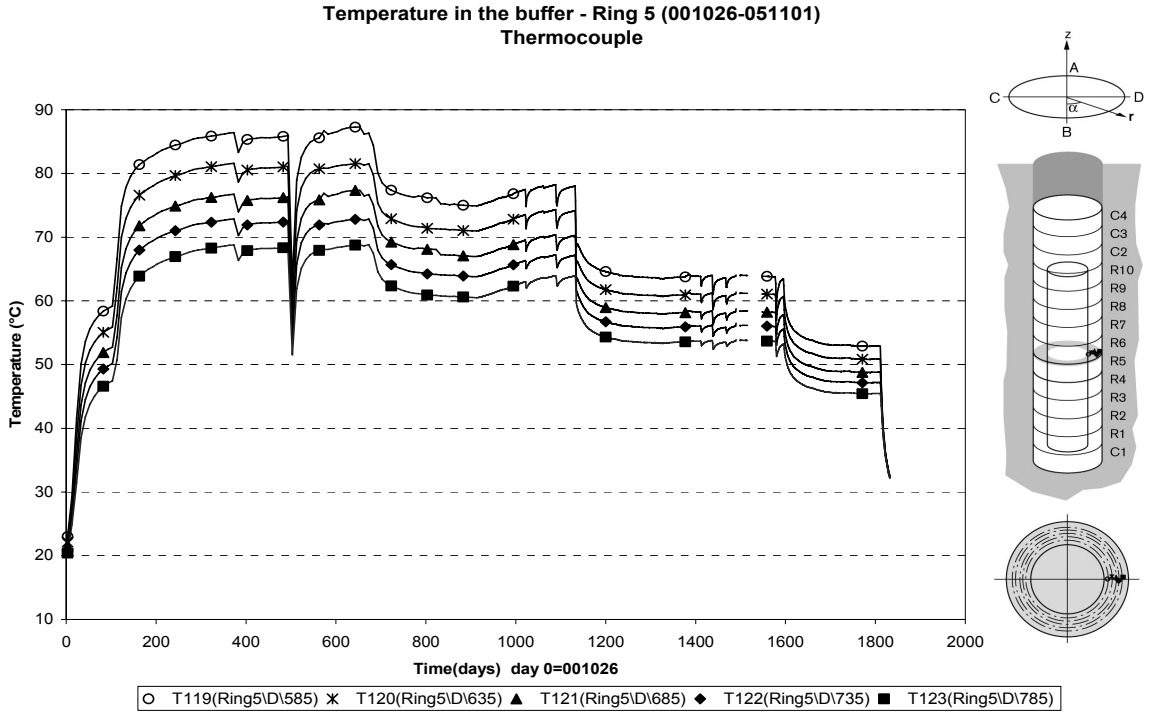

Figure 3-4. *Measured temperature in the bentonite ring5/from Reza and Lennart 2005/.*

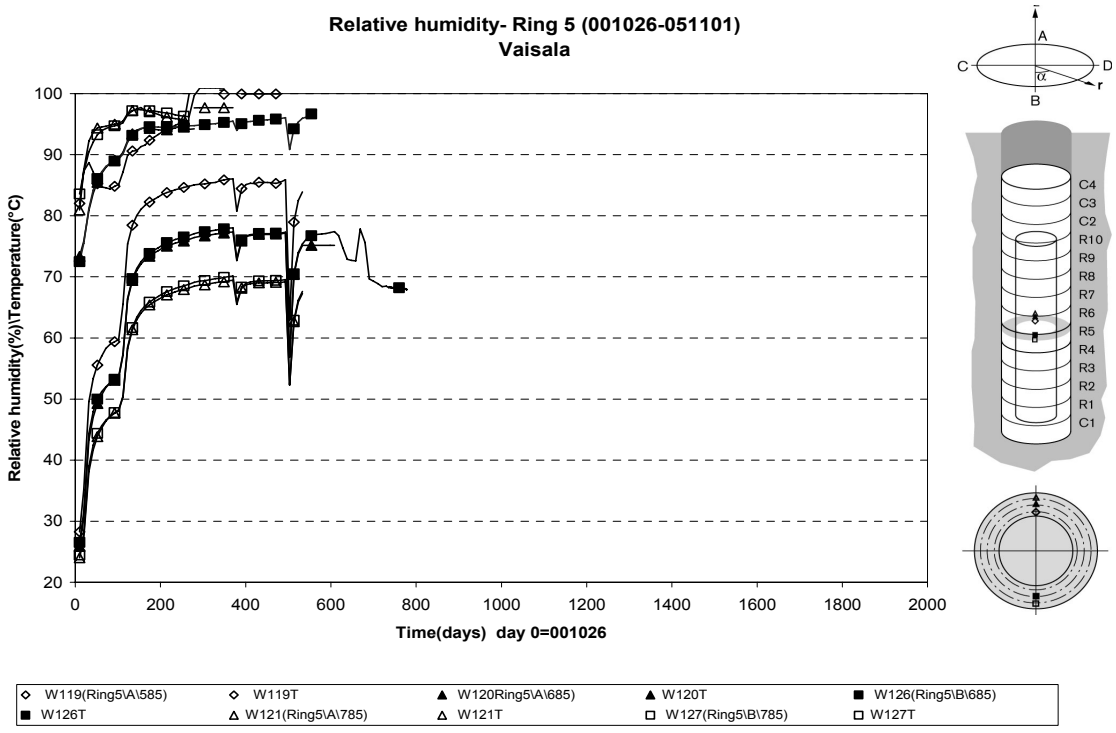

Figure 3-5. *Measured relative humidity in the bentonite ring 5/from Reza and Lennart 2005/.*

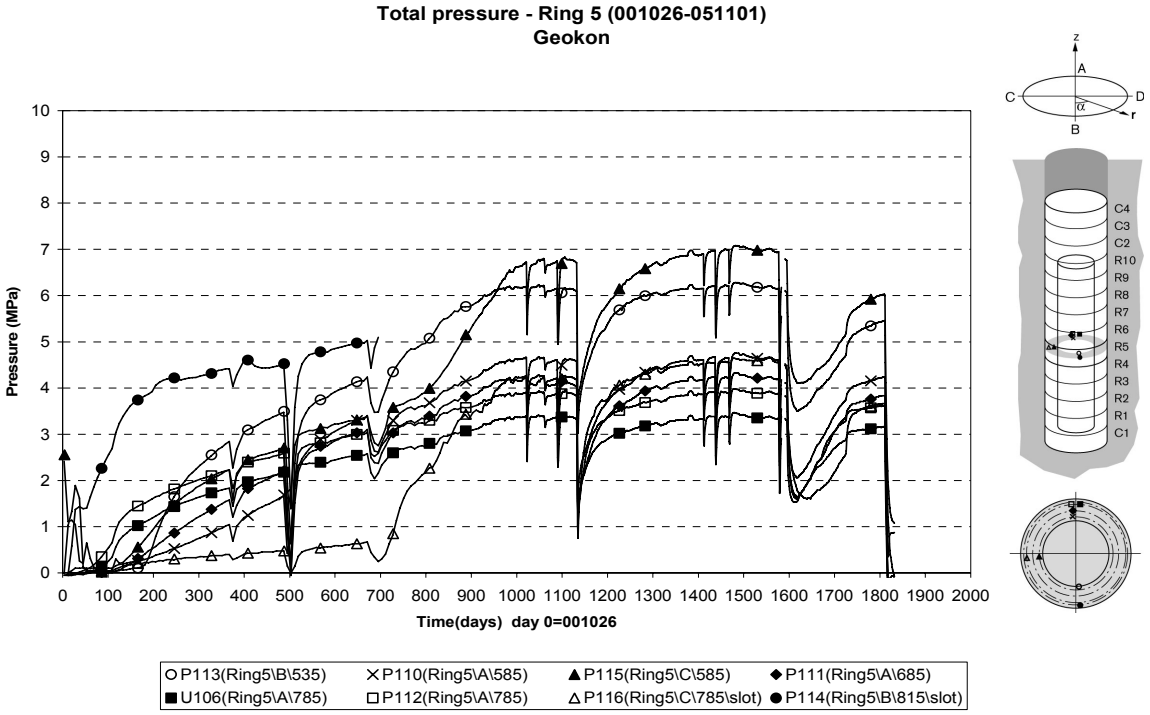

Figure 3-6. *Measured total pressure in the bentonite ring 5/from Reza and Lennart 2005/.*

Figure3-4 shows that the temperature in the bentonite ring responded nearly instantaneously to the variation of heat load and decreased with the increase of distance to the canister. The maximum temperature near the rock in this ring was about 70^0C and was reached on day 350 or so. The relative humidity, as can be seen from Figure 3-5, was over 90% about 30 days after the start and over 95% after about 100 days and the transducers failed to yield reasonable results after about 500 days, which probably was due to higher relative humidity and degree of saturation. It can be seen from Figure 3-6 that the total pressures at all points had the overall tendency to increase until about 1600days and were higher than 3MPa at the end of CRT on day 1811. On about day 683, when the heat power was reduced from its maximum values of 2600W to 2100W, the total pressure near the rock in ring 5 was 3 to 5MPa, with the exception measured by P116. The total pressures measured at the bottom of the hole were higher than those in ring5, with the maximum value of 7MPa and had the value of about 4–6MPa near the rock on day 683 and greater than 4MPa at the end of CRT on day 1811.

3.5 Measured temperature in the rock

Figure3-7 to Figure3-9 are the results of temperature measurements in the rock at three depths: 3.5m, 5.5m and 7.9m, corresponding to the top, the middle and the bottom of the canister, respectively. It can be seen that the temperature at depth 5.5m (Figure3-8) was higher than that at depth 7.9m (Figure3-9), the latter was slightly higher than that at depth 3.1m (Figure3-7). The maximum value of measured temperature in the rock was about 65^0C. The temperature reaction to the heating was quite similar among the three directions before the TBT heating started. After that, it became anisotropic due to

different influence from TBT. There were two peaks for the measured volume: one corresponding to the end date of CRT maximum heat power at about day 683 and the other corresponding to the date at about day 1135when the CRT heat power was reduced from 2100W to 1600W and TBT heating had started. For rock near the CRT hole wall, the two peaks approximately had the same value, but for rock out of the CRT wall on the TBT side, the second peak was higher than the first one. The temperatures in the rock near the hole wall on day 1811 were about 40–45^{0}C at depth 5.5m and 35–40^{0}C at depth 3.1m and 7.9m.

3.6 Visual observation of the CRT hole

A careful observation of the CRT deposition hole surface after the experiment ended shows that no obvious change and visible damage could be found. See Figure 3-10 for comparison.

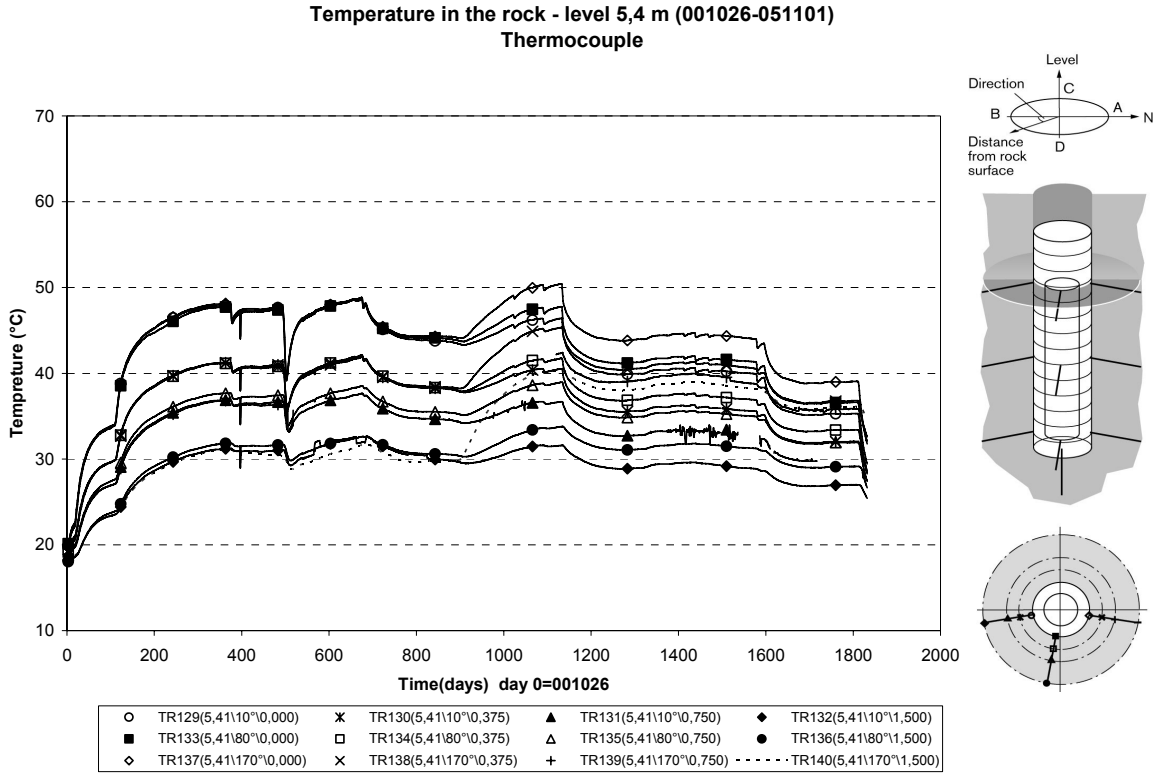

Figure 3-7. *Temperature in the rock–depth 3.1m/from Reza and Lennart 2005/.*

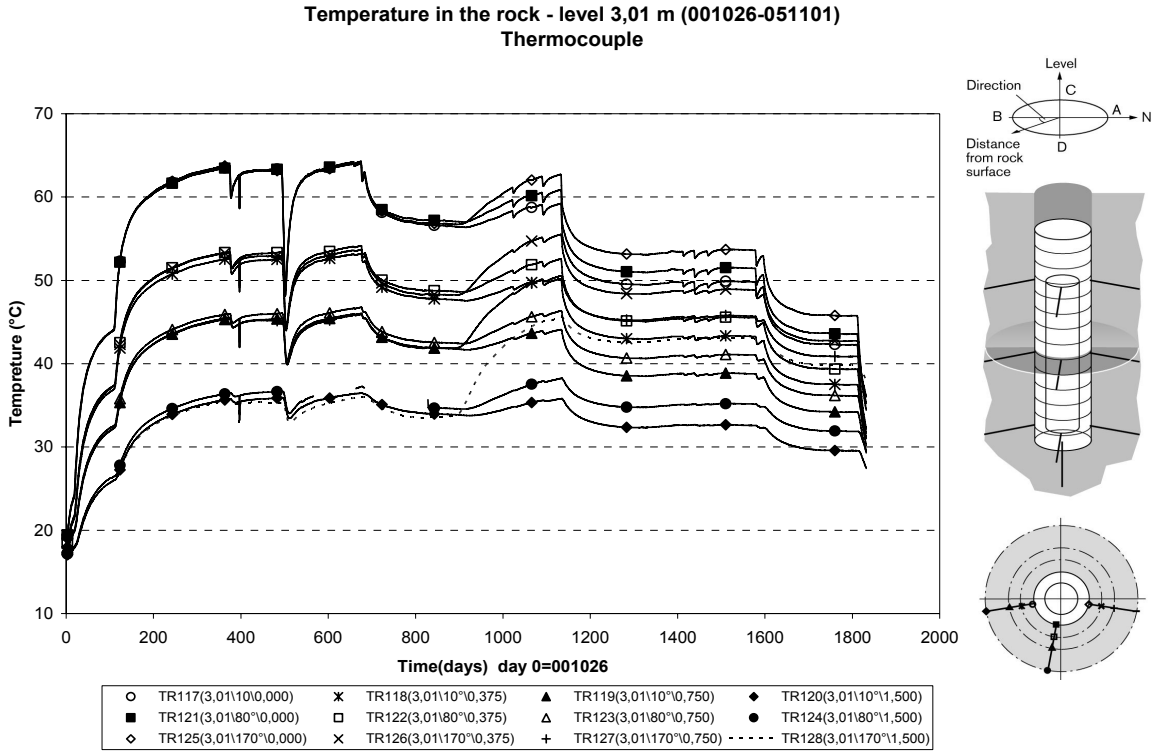

Figure 3-8. *Temperature in the rock–depth 5.5m/from Reza and Lennart 2005/.*

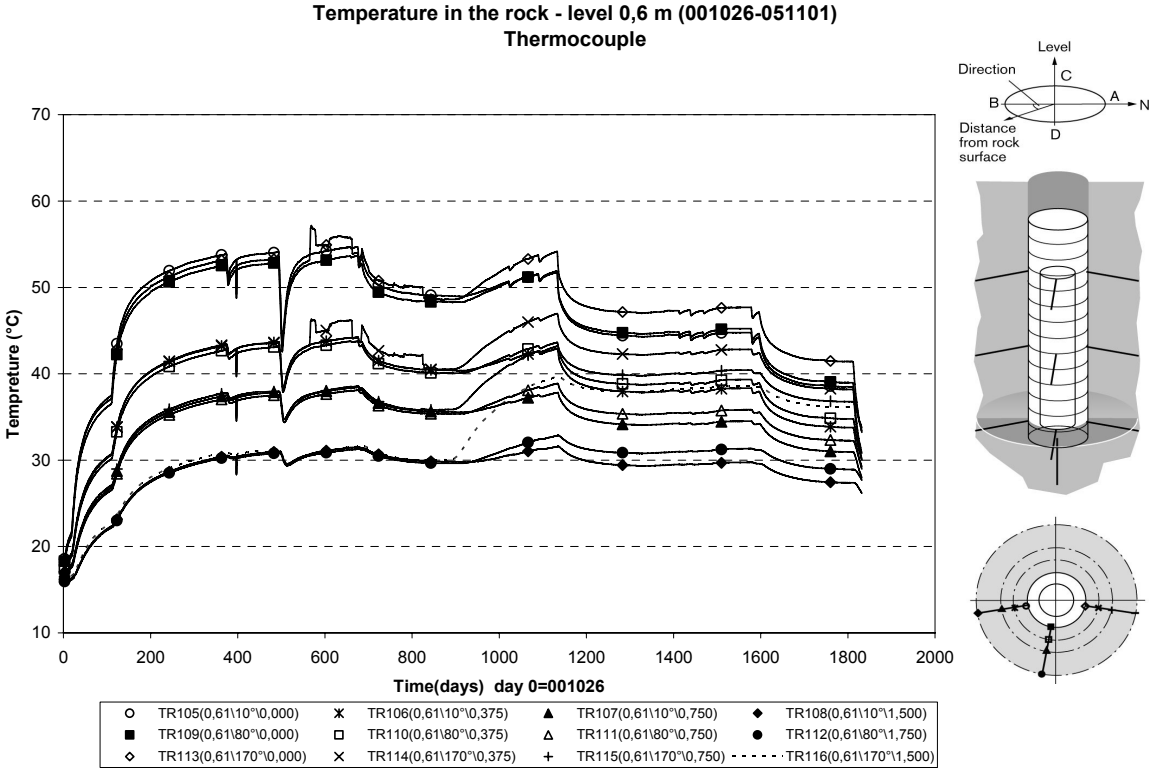

Figure 3-9. *Temperature in the rock–depth 7.9m/from Reza and Lennart 2005/.*

(a) before experiment

(b) after experiment

Figure3-10. *Photographs of DD0092G01surface before and after experiment.*

4 Analysis of UCS testing results

4.1 Samples description

After the CRT, 6 sub-horizontal core boreholes were drilled about 1.5m into the rock from the rock wall of the CRT deposition hole (DD0092G01) at three depths, 3.4m, 6.0m and 7.9m, respectively, counting from the tunnel floor. The holes had been drilled parallel and perpendicular to the direction of the major principal stress to make the maximum and minimum loaded parts of the rock sampled.

The general geological mapping of the cores from these holes, including rock types, zones of alteration, sealed and open fractures, was performed. With the help of core mapping, 2 core samples from each borehole, one from the beginning part and the other from the end part, were taken. In total, 12 core samples were collected. Thus, rocks loaded to maximum and minimum stress and heated to higher and lower temperature had been sampled.

The location details and description of these samples can be seen from Table 4-1 and Figure 4-1. Figure 4-2 and Figure 4-3 are photographs of specimens taken from the 6 core boreholes about 0.15m and 1.5m from the deposition hole wall, respectively. It can be found from Table 4-1 and Figure 4-2 to 3 that the samples belong to two rock types: samples from the upper part of the deposition hole wall (samples from KD0092G17, G18, G20, G21) are greenstone, whereas samples from the lower part are Äspö diorite. Some foliations were found in samples taken from KD0092G20 and KD0092G21 and some veins or inclusions of granite were seen in some samples. As a whole, samples collected from different directions and different parts of the core boreholes show no obvious geological difference.

4.2 Experimental method

The Uniaxial Compression Tests were executed according to the method description SKB MD 190.001e version3.0 (Method Description for Uniaxial Compression Test). The test specimens were water-saturated according to the method description SKB MD160.002e version 2.0.

In all uniaxial compression tests, the acoustic emission was monitored with an independent system not interfering with the uniaxial compression test to estimate crack initiation and crack damage stress depths. Acoustic emission measurement followed methodology developed for Posiva site investigations (Hakala & Heikkilä 1997).

The testing report is attached in Appendix 1.

Table 4-1 Samples´ locations and rock type

Borehole number	Sample Number*	Direction**	Depth (m)	Distance (m)***	Rock description
KD0092G17	G17-113-1	N40^{0}E (perpendicular to σ_1)	3.4	0.03-0.18	Greenstone, mid-grained, with inclusion of granite
	G17-113-2			1.55-1.70	Greenstone, homogenous
KD0092G18	G18-113-1		6.0	0.03-0.18	Greenstone, mid-coarse grained, with some inclusion of granite
	G18-113-2			1.40-1.55	Greenstone, homogenous
KD0092G19	G19-113-1		7.9	0.04-0.19	Äspö diorite, with veins of fine-grained granite
	G19-113-2			1.49-1.64	Äspö diorite
KD0092G20	G20-113-1	N310^{0}E (parallel to σ_1)	3.4	0.06-0.21	Greenstone, with veins of fine-grained granite, slightly foliated
	G20-113-2			1.55-1.70	Greenstone, with inclusion of granite, slightly foliated
KD0092G21	G21-113-1		6.0	0.07-0.22	Greenstone, mid-coarse grained, with inclusion of granite and foliation
	G21-113-2			1.60-1.75	Greenstone with foliation
KD0092G22	G22-113-1		7.9	0.06-0.21	Äspö diorite
	G22-113-2			1.25-1.40	Äspö diorite

*: The sample number hereinafter will be written as G17-1 for KD0092G17-113-1 and so on, if necessary for simplification.

**: The direction hereinafter will be written as perpendicular (perp. in short if necessary) and parallel (para in short if necessary) for N40^{0}E and N310^{0}E respectively.

***: The distance to the hole wall will hereinafter be simply distinguished as start and end for samples near to and about 1.5m away from the hole wall.

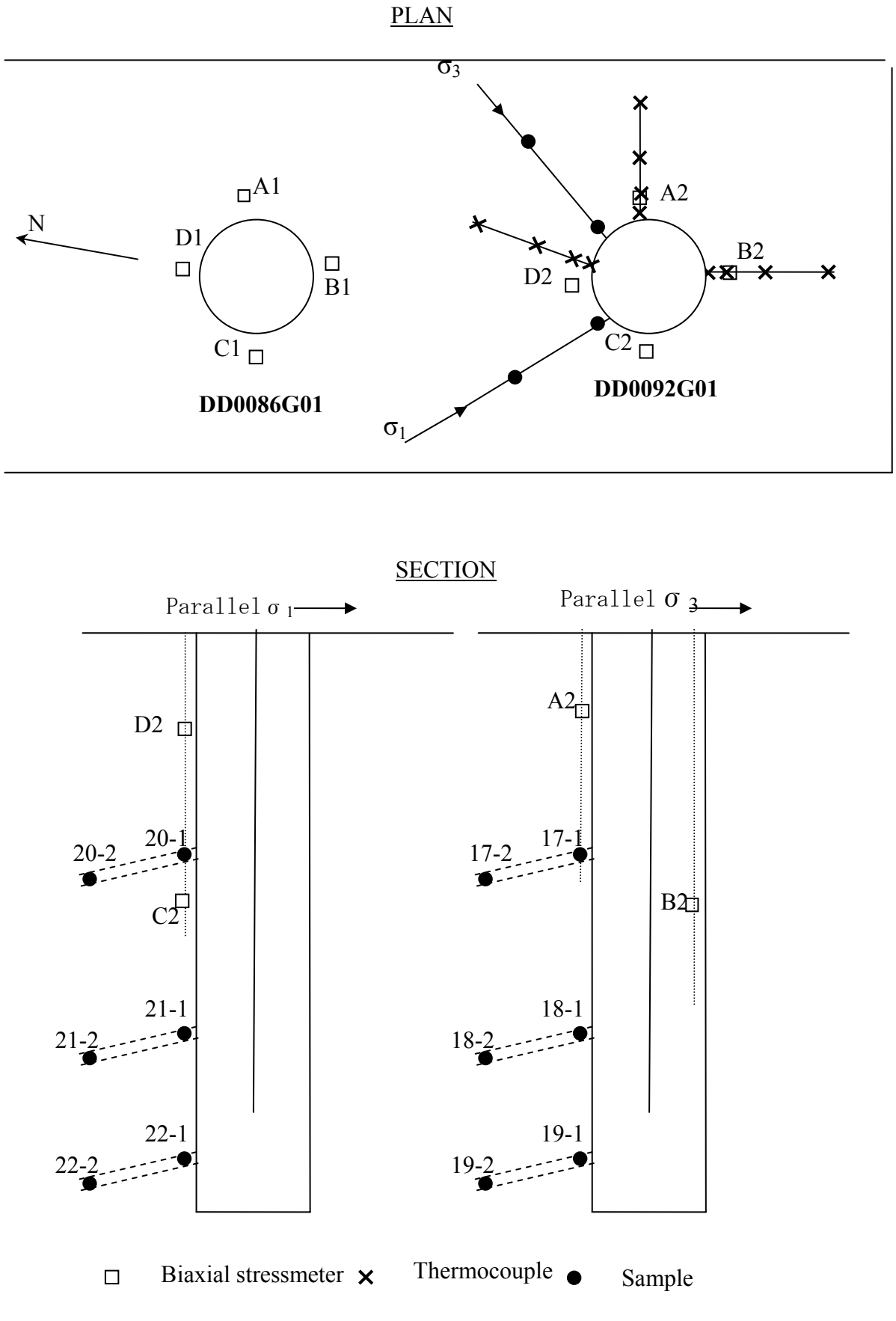

Figure 4-1. *Schematic drawing of the samples location.*

G17-113-1 G18-113-1 G19-113-1

G20-113-1 G21-113-2 G22-113-1

Figure 4-2. *Photographs of specimen taken from the deposition hole wall.*

G17-113-2

G18-113-2

G19-113-2

G20-113-2

G21-113-2

G22-113-2

Figure 4-3. *Photographs of specimen takenfrom about 1.5m away from the deposition hole wall*

4.3 Experimental results and analysis

4.3.1 UCS and elastic properties

Table 4-2 presents the rock mechanical properties obtained from uniaxial compression test. Figure 4-4 shows the results of UCS and Young´s modulus and comparison of average UCS and Young´s modulus with the typical values for Äspö HRL and from ASPE. Figure 4-5 and 4-6 are histograms showing the comparison of UCS and Young´s modulus according to sampled directions and distance, whereas Figure4-7 and Figure4-8 show the mean values and variation coefficient of UCS and Young´s modulus for different combinations of samples, respectively.

Table 4-2. Rock mechanical properties measured by UCS testing

Sample number	UCS (MPa)	Young´s modulus (GPa)	Poisson´s ratio	Failure mode
G17-113-1	123.2	56.3	0.34	Axial cleavage
G17-113-2	108.5	50.8	0.32	Vertical splitting
G18-113-1	146.0	61.7	0.34	Axial cleavage
G18-113-2	115.2	53.5	0.35	Axial cleavage
G19-113-1	170.1	65.6	0.31	Axial cleavage
G19-113-2	149.6	59.5	0.34	Axial cleavage
G20-113-1	88.3	58.2	0.27	Vertical splitting
G20-113-2	121.5	59.6	0.33	Axial cleavage
G21-113-1	124.1	62.1	0.30	Axial cleavage
G21-113-2	91.3	63.3	0.27	Vertical splitting and shear
G22-113-1	155.3	66.3	0.30	Axial cleavage
G22-113-2	134.2	66.0	0.30	Axial cleavage
total				
mean	127.3	60.2	0.31	
standard deviation	25.0	4.9	0.03	
Greenstone				
Mean(all)	114.8	58.2	0.32	
standard deviation(all)	18.8	4.4	0.03	
Mean(a.c.)	126	58.6	0.33	
Standard deviation(a.c)	11.7	3.7	0.02	
Äspö diorite				
mean	152.3	64.4	0.31	
standard deviation	14.8	3.2	0.02	
Greenstone(typical)				
Mean	207	78	0.24	
Standard deviation	53	10		
Äspö diorite(typical)				
	171	73	0.24	
	35	4		
Äspö diorite(APSE)				
Mean	211	73.8	0.25	
Standard deviation	23	3.6		

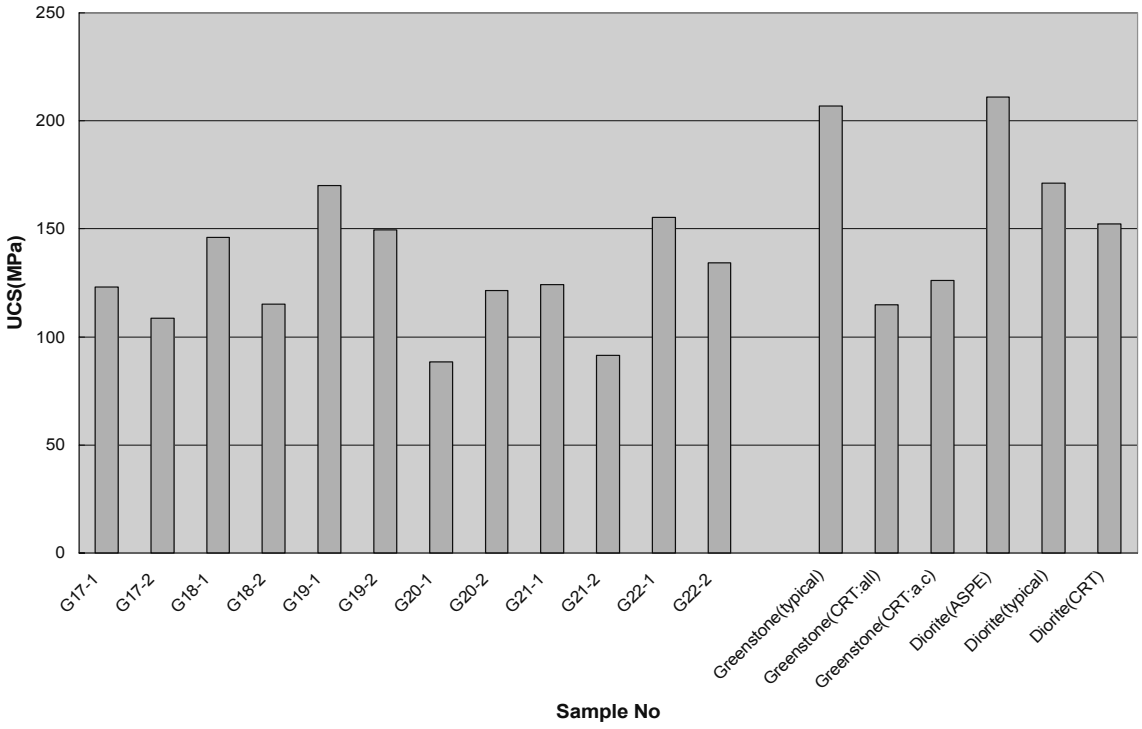

(a) UCS

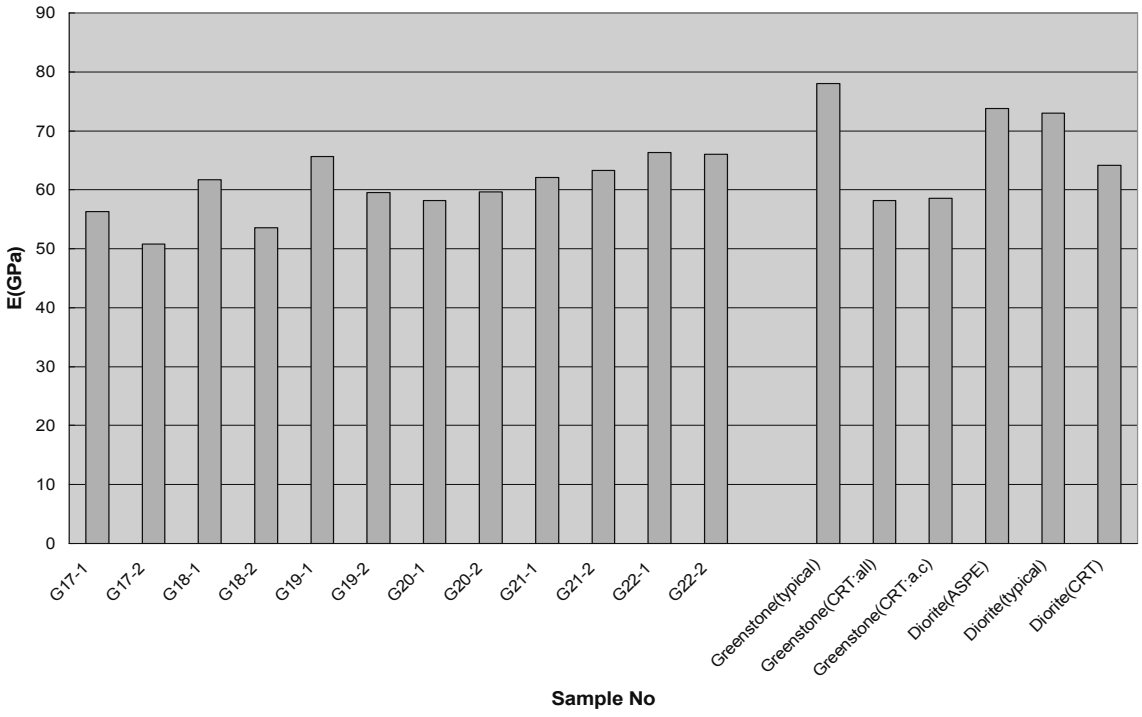

(b) Young´s modulus

Figure 4-4. *Histogram of UCS and Young´s modulus of all samples and comparison with other locations at Äspö*

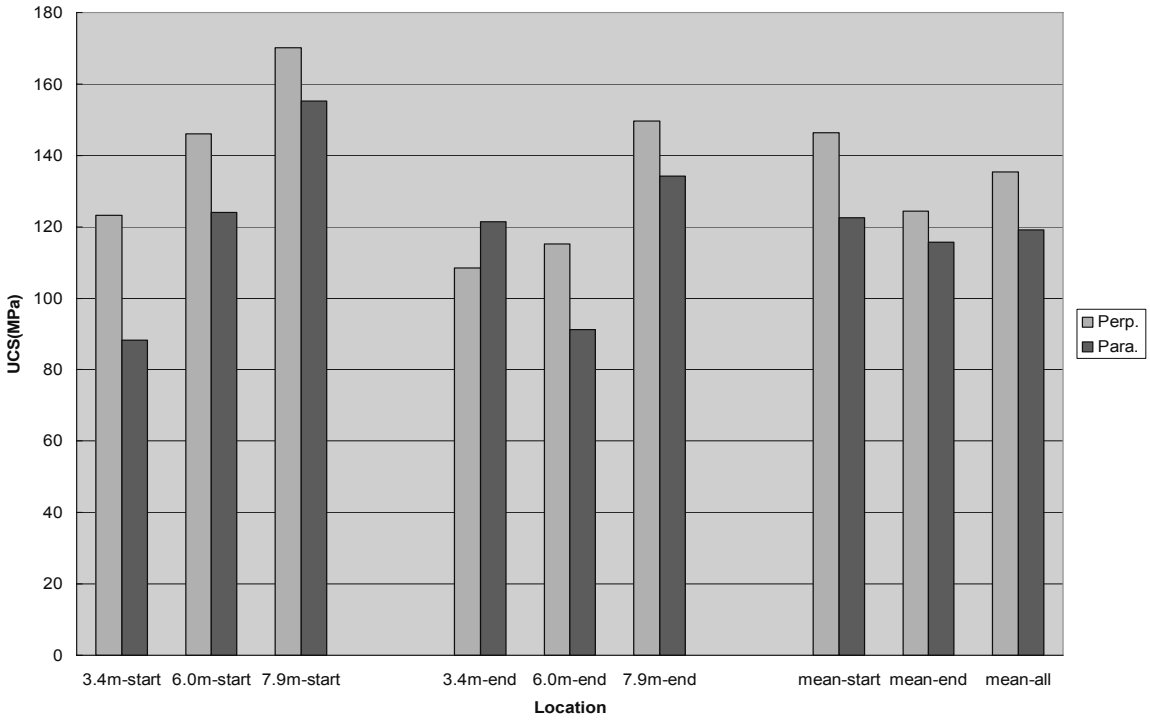

(a) UCS

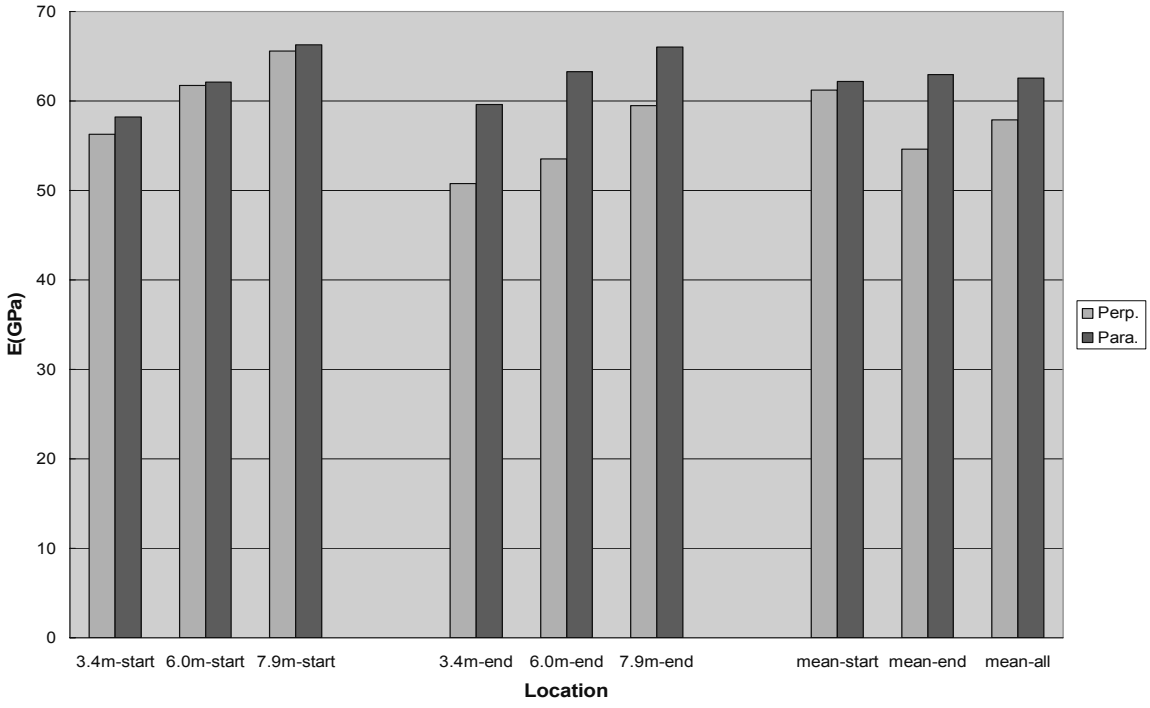

(b) Young´s modulus

Figure 4-5. *Comparison of UCS and Young´s modulus between samples from the direction parallel and perpendicular to major principal stress.*

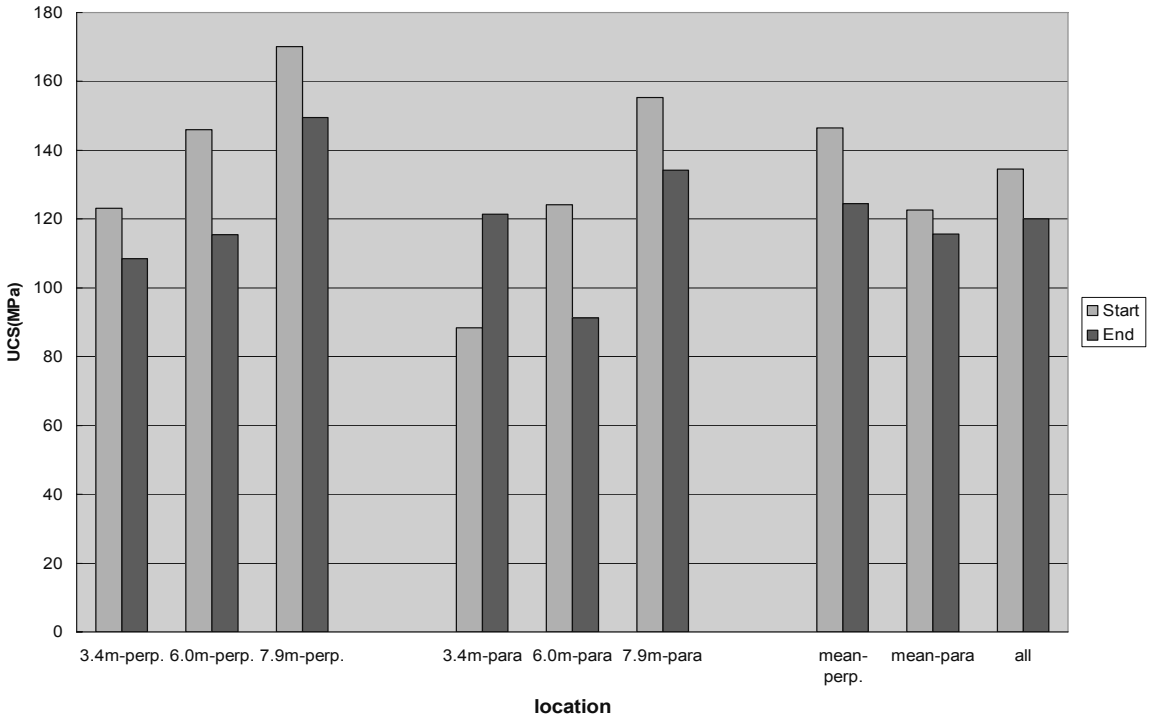

(a) UCS

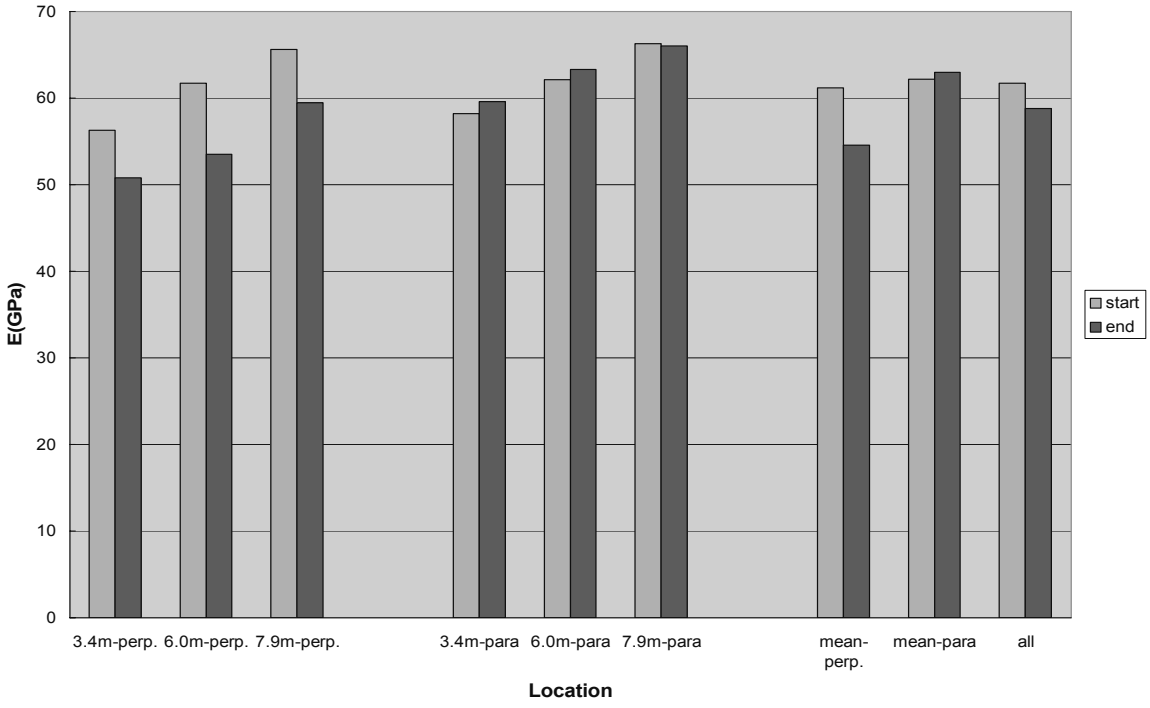

(b) Young´s modulus

Figure 4-6. *Comparison of UCS and Young´s modulus according to the distance to the deposition hole wall.*

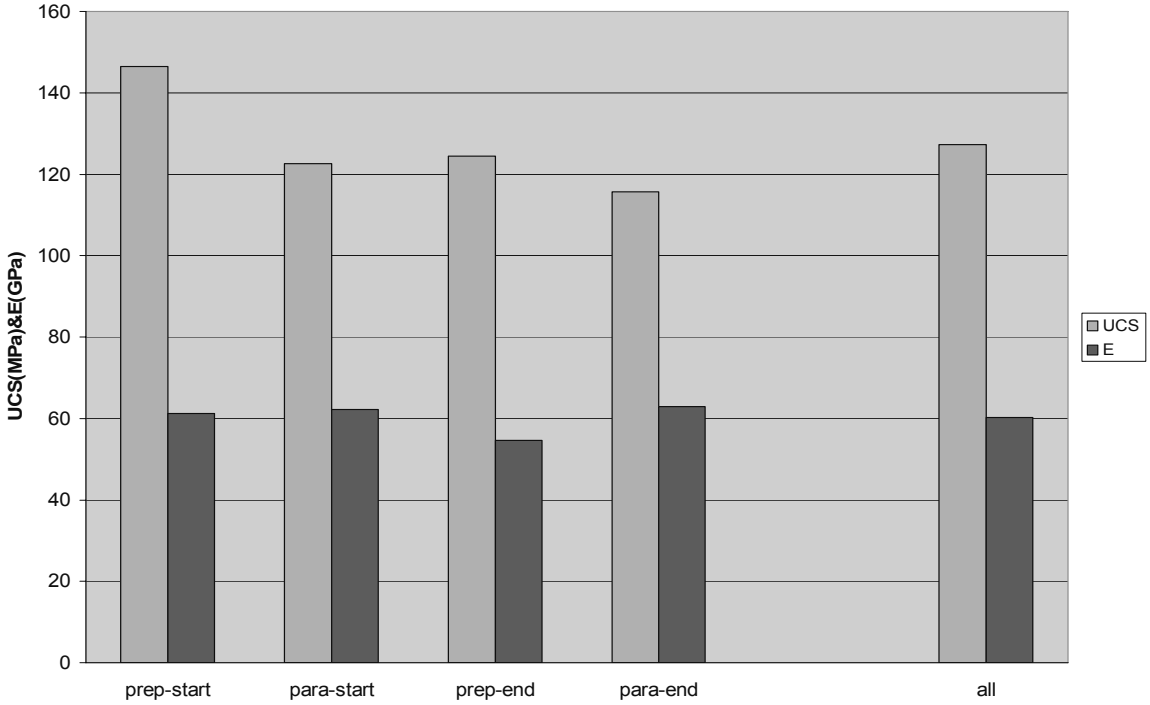

Figure4-7. *The average values of UCS and Young´s modulus for different combination of direction and distance and comparison with that for all samples.*

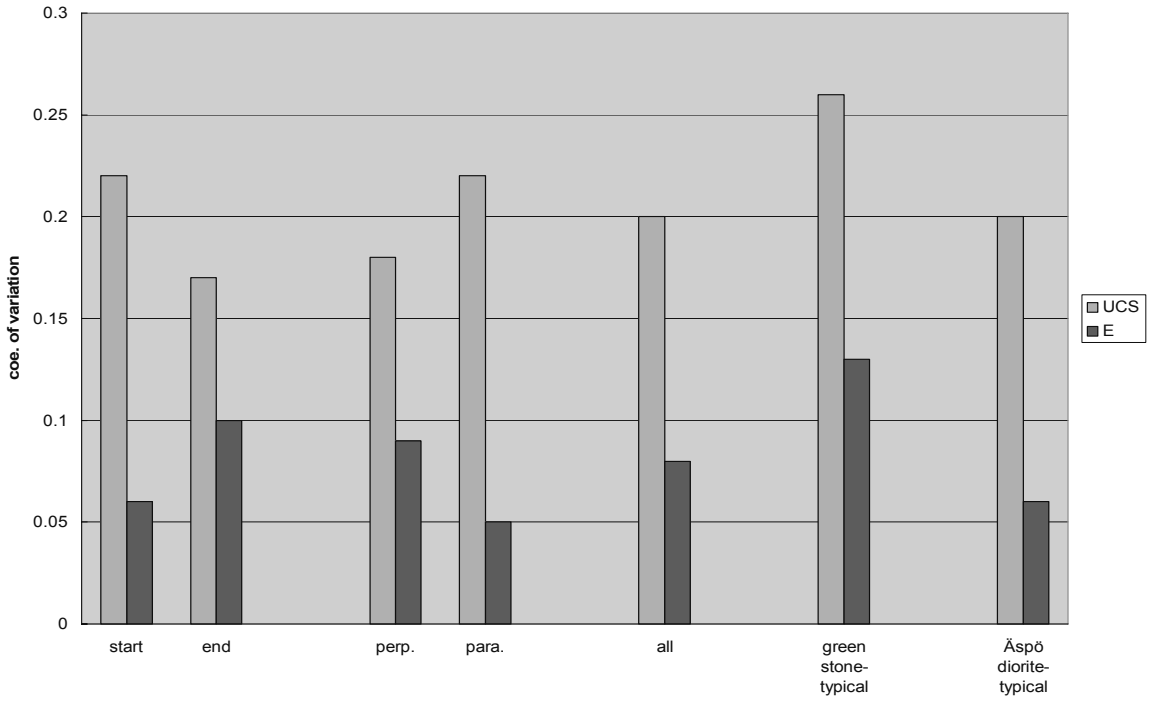

Figure4-8. *Coefficient of variation for different combination of samples and comparison with that for all samples.*

It can be found from Table 4-2 and Figure 4-4 through Figure 4-8 that:

(2) As shown in Table 4-2 and Figure 4-4, compared with the typical values of the same rock type at Äspö HRL and the data from ASPE, both greenstone and diorite surrounding CRT deposition hole have a lower strength and higher deformation. The Poisson´s ratio exhibits very small variation, but their values are a little higher than the typical value at Äspö HRL.

(3) As shown in Table 4-2 and Figure 4-4, the rock Äspö diorite has a higher strength than the greenstone.

(4) Some samples with foliation failed as axial splitting and exhibited lower UCS, as listed in Table 4-2.

(5) In terms of UCS, as shown in Figure 4-5(a), except core borehole G20, the samples collected in the direction perpendicular to the major principal stress are slightly stronger than samples in the parallel direction; and as shown in Figure 4-6(a), except core borehole G20, samples from the starting part of the core borehole(nearest to the deposition hole wall), have slightly higher strength than samples from the end part of the core boreholes(about 1.5m away from the deposition hole wall). It can also be found from Figure 4-7 that, among the four combinations according to sample direction and distance, the combination of samples collected near the deposition hole wall in the direction perpendicular to major principal stress has the highest average UCS and the other three groups of combinations have very near average UCS values. Therefore, it seems that the rock in the inner part, which experienced higher temperature during heating stage, and the rock in the direction perpendicular to major principal stress, which were maximum loaded during excavation and heating stage, is stronger.

(6) In terms of Young´s modulus, when compared according to the sampled direction, as shown in Figure 4-5(b), the tendency is that samples taken near the deposition hole wall of the same depth have almost the same value, but for samples taken about 1.5m away from the deposition hole wall, samples collected in the direction perpendicular to the major principal major stress have lower value than those from the parallel direction. If compared according to the sample´ distance to the deposition hole, Figure 4-4(b) and 4-6(b) show that, in the direction perpendicular to the major principal major, samples near the deposition hole wall have higher values of Young´s modulus than those about 1.5m away, however, in the direction parallel to the major principal stress, samples at the same depth have approximately same value. Figure 4-7 shows that the average value of Young´s modulus for samples collected about 1.5m to the deposition hole wall in the direction perpendicular to major principal stress is the lowest, and all the other three combinations have very similar average values of Young´s modulus.

(7) As shown in Figure 4-8, the coefficients of variation are less than 0.25 for UCS and 0.10 for Young´s modulus, which are comparable to those for Äspö HRL. As a whole, the scatter in UCS and Young´s modulus is small. Compared according to sample´ distance, the samples collected near the deposition hole wall have slightly higher variation coefficient of UCS but relatively lower variation coefficient of Young´s modulus. The samples from the direction perpendicular to major principal stress have slightly lower variation coefficient of UCS but relatively higher variation coefficient of Young´s modulus than those from parallel direction.

4.3.2 Crack initiation stress and crack damage stress

During the elastic stage of unaxial compression tests, the total volumetric strain ε_v, the elastic volumetric strain ε_{ve} and the crack volumetric strain ε_{vc} can be calculated from the following expressions:

$$\varepsilon_v = \varepsilon_a + 2\,\varepsilon_r \qquad (2.1)$$

$$\varepsilon_{ve} = \sigma(1-2\upsilon)/E \qquad (2.2)$$

$$\varepsilon_{vc} = \varepsilon_v - \varepsilon_{ve} \qquad (2.3)$$

Where ε_a and ε_r are axial radial strain, and E and υ are Young´s modulus and Poisson´s ratio, respectively.

Crack damage stress(CDS) can be determined from the curve of total volumetric strain versus axial stress, and the crack initiation stress (CIS) can be identified from the reversal point of the curve of crack volumetric strain versus axial stress. In addition, the crack damage stress (CDS) and crack initiation stress (CIS) can also be determined from the intensity of Acoustic Emission (AE) events recorded versus axial stress by defining the initiation of micro-cracking as the crack initiation stress (CIS) and beginning of unstable micro-cracking as crack damage stress(CDS).

Results of crack stresses from UCS and AE are listed in Table 4-3.

Table 4-3. Summary of crack initiation stress (CIS) and crack damage stresses (CDS)

Sample number	Crack stress from UCS (MPa)		Crack stress from AE (MPa)		CIS/UCS	
	CIS	CDS	CIS	CDS	From UCS	From AE
G17-113-1	60	100	75	120	0.48	0.61
G17-113-2	55	85	70	108	0.51	0.65
G18-113-1	70	115	75	140	0.48	0.51
G18-113-2	60	90	60	115	0.52	0.52
G19-113-1	85	140	80	165	0.50	0.47
G19-113-2	78	115	75	145	0.52	0.50
G20-113-1	45	85	75	85	0.51	0.85
G20-113-2	65	100	80	120	0.54	0.66
G21-113-1	60	110	80	120	0.48	0.65
G21-113-2	45	70	65	70	0.49	0.72
G22-113-1	78	135	80-90	140	0.50	0.52-0.58
G22-113-2	71	120	80	130	0.53	0.60
Mean standard deviation	64.1 12.7	105.4 21.0	74.1 7.1	121.5 26.0	0.51 0.02	0.61 0.11
Greenstone mean standard deviation	 57.5 8.8	 94.4 14.7	 72.5 7.1	 109.8 22.2	 0.50 0.02	 0.65 0.11
Äspö diorite mean standard deviation	 78 5.7	 127.5 11.9	 78.3 4.1	 145 14.7	 0.51 0.02	 0.52 0.04
ASPE –Åspö diorite mean Standard deviation	 96.1 12.0	 201.8 30.4	 121 31.3	 204 15.6		

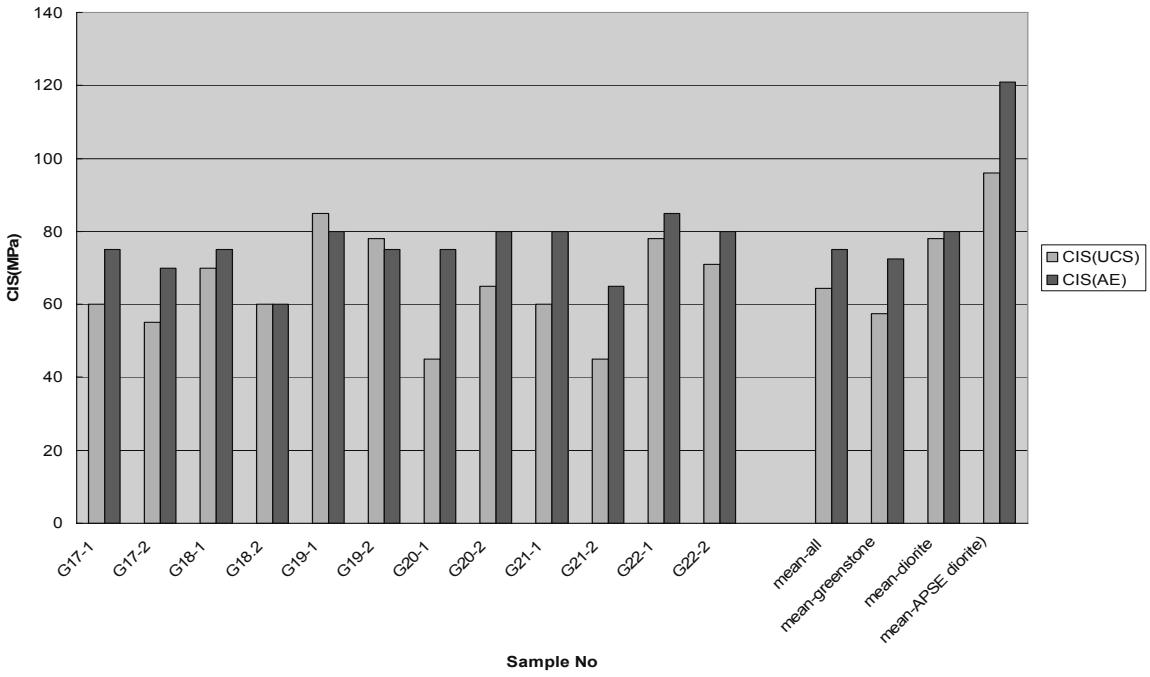

(a) CIS

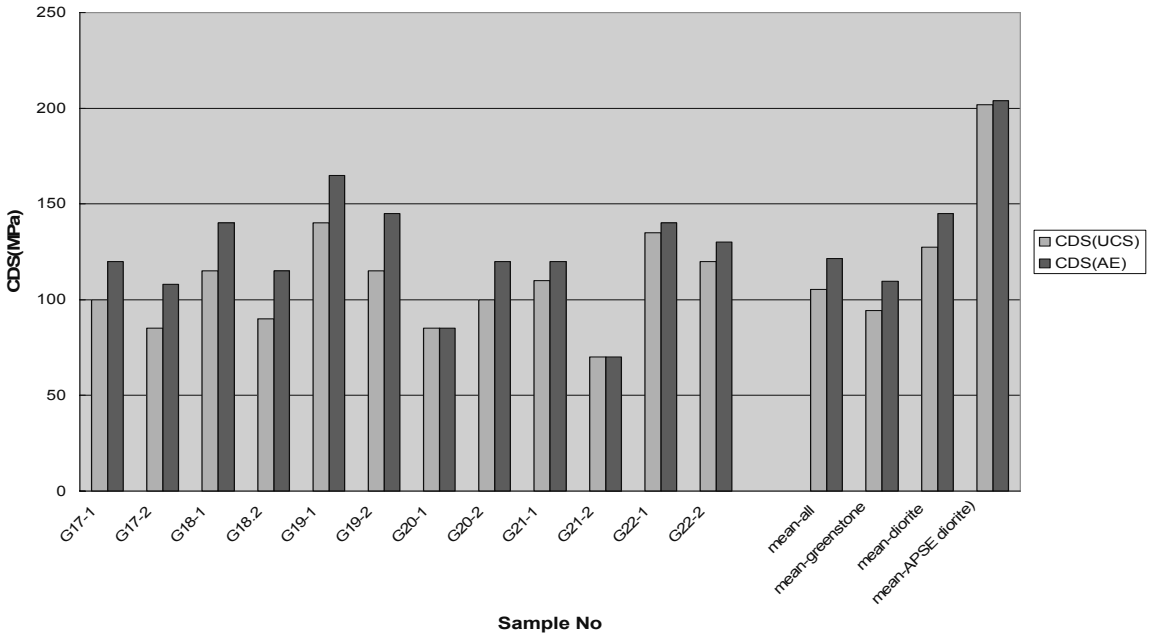

(b) CDS

Figure 4-9. *Histogram of CIS and CDS of all samples and comparison with other locations at Äspö.*

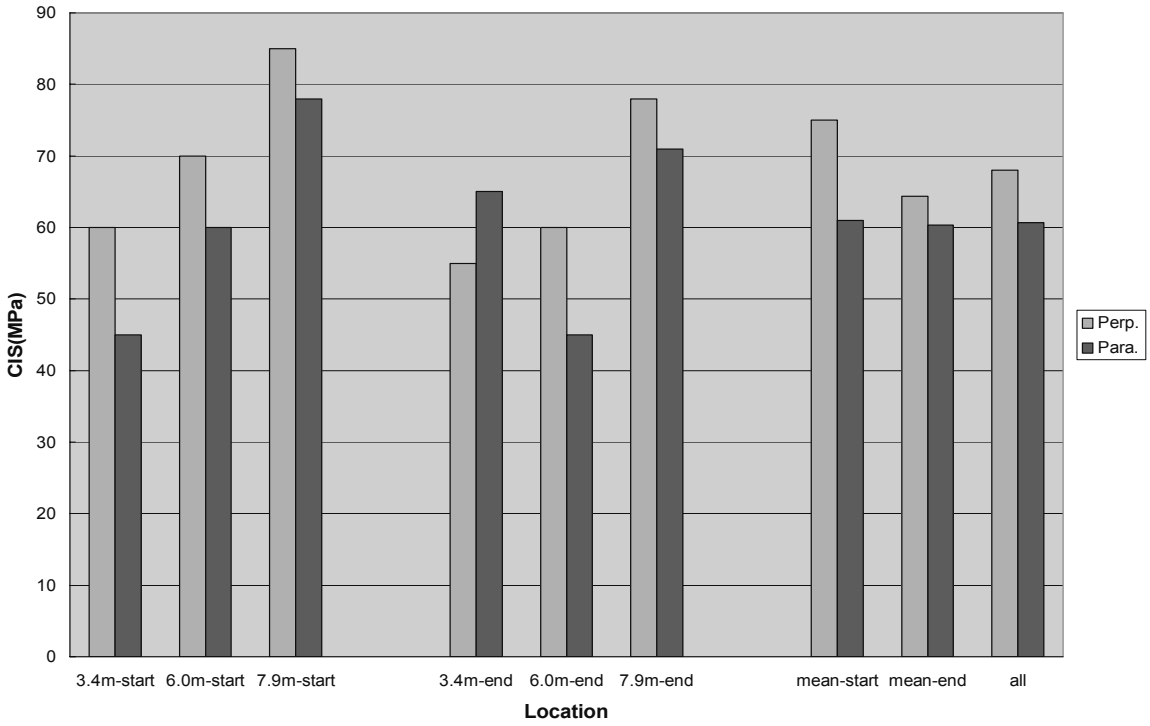

(a) from UCS

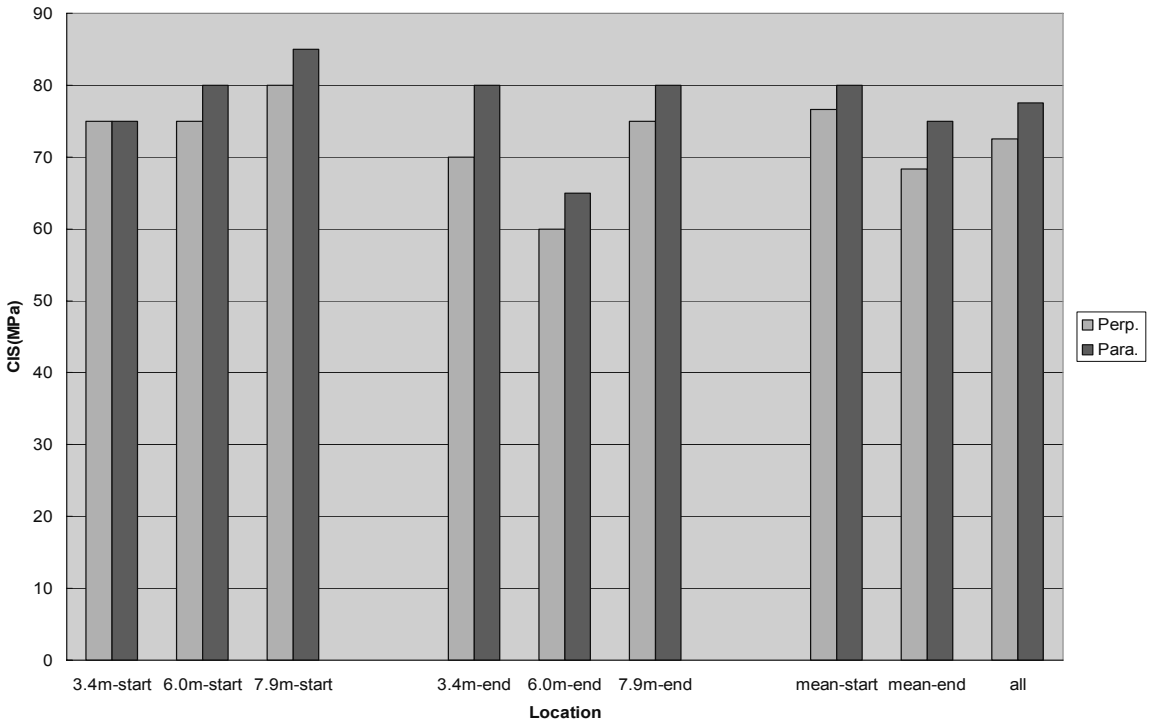

(b) from AE

Figure 4-10. *Comparison of CIS between samples from the direction parallel and perpendicular to major principal stress.*

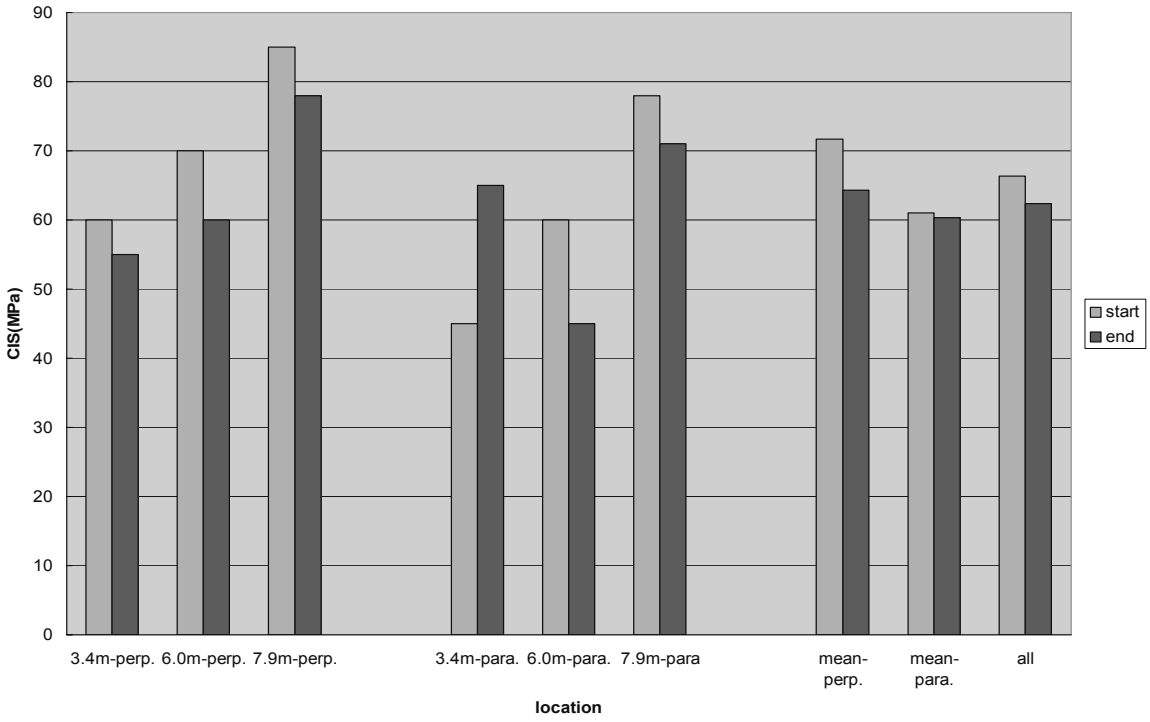

(a) from UCS

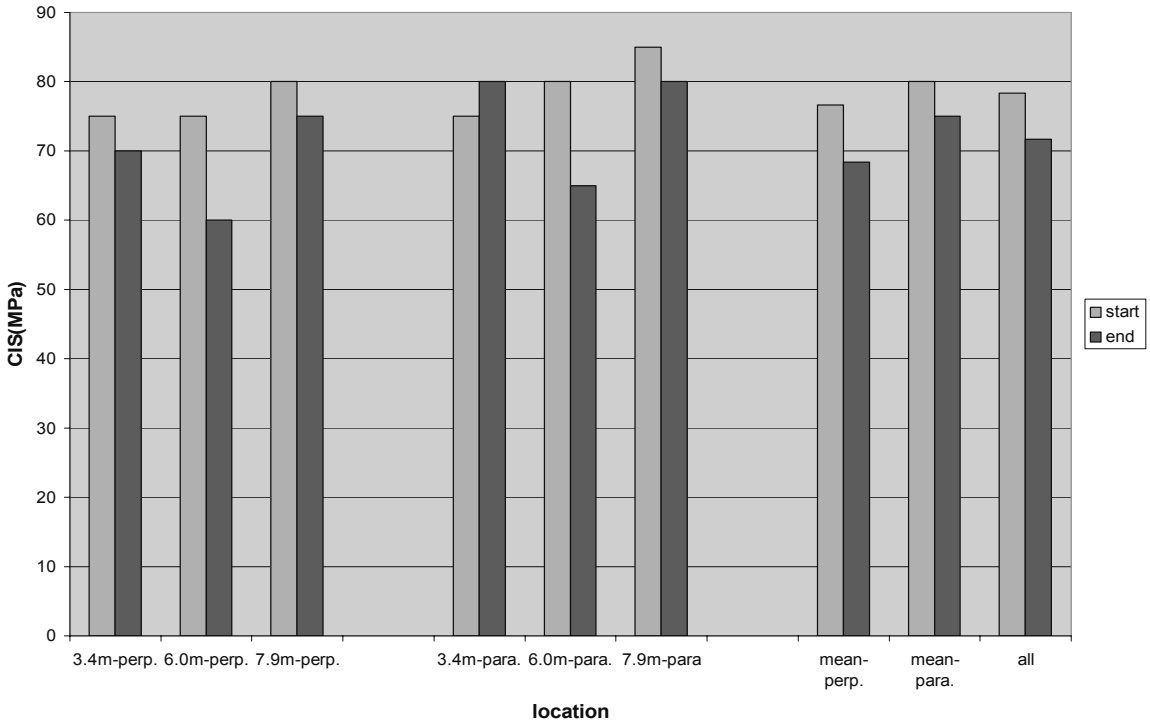

(b) from AE

Figure 4-11. *Comparison of CIS according to the distance to the deposition hole wall.*

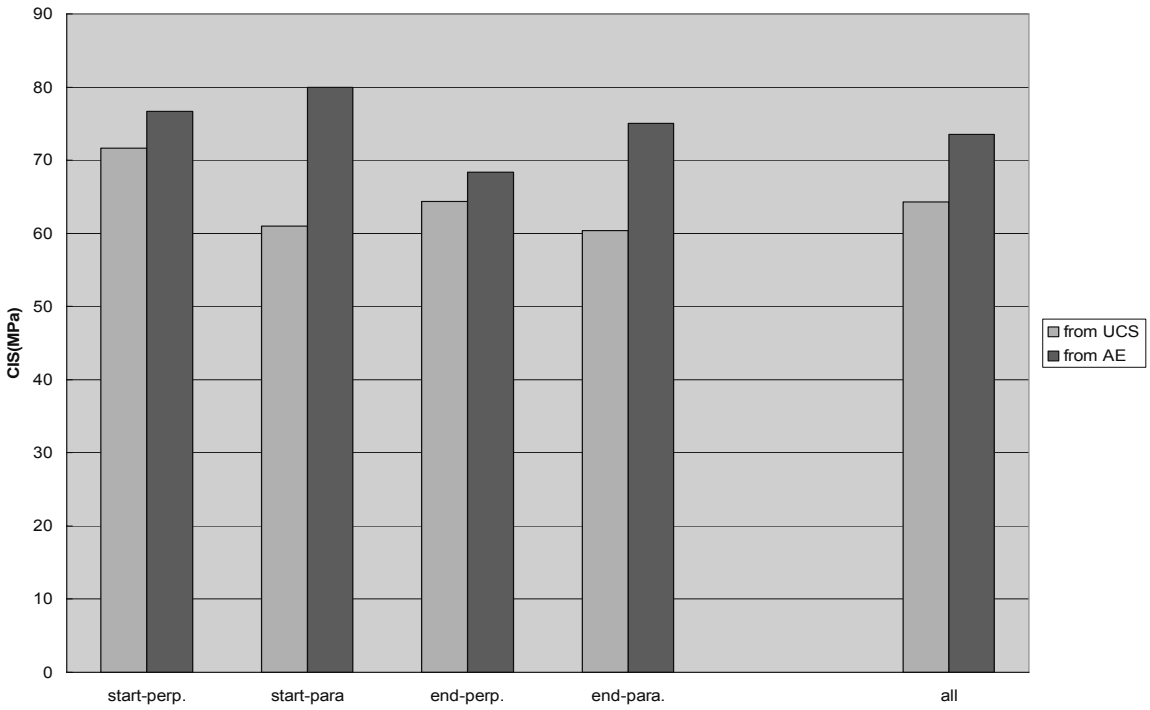

Figure 4-12. *The average values of CIS for different combination of direction and distance and comparison with that for all samples.*

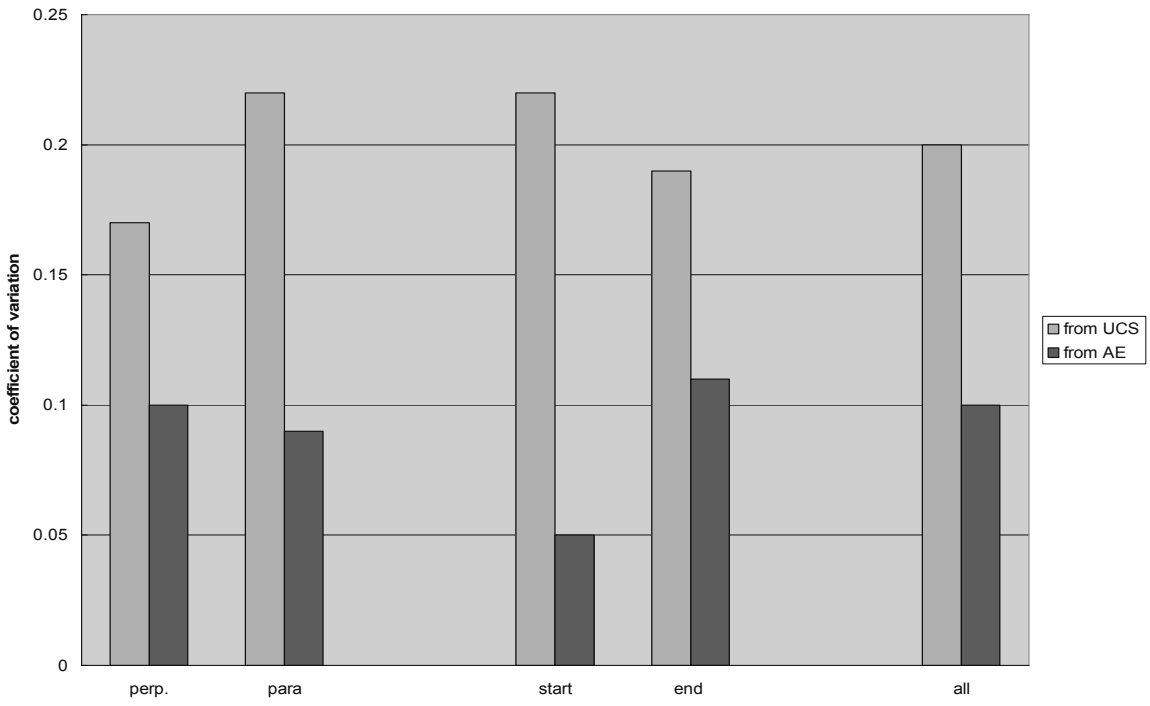

Figure 4-13. *CIS coefficient of variation for different combination of samples and comparison with that for all samples.*

It can be found from Table 4-3 and Figure 4-9 through Figure 4-13 that:

(1) As shown in Table 4-3 and Figure 4-9, compared with data from ASPE, Äspö diorite in the CRT deposition hole has a lower crack initiation stress and crack damage stress.

(2) Table 4-3 and Figure 4-9 show that crack initiation stress and crack damage stress determined by AE are higher than those from UCS testing.

(3) Äspö diorite in the CRT has higher crack initiation and crack damage stresses than the greenstone, as indicated in Table 4-3 and Figure 4-9.

(4) From UCS testing results, as shown in Figure 4-10(a), samples(except those fromG20) from the direction perpendicular to major principal stress have slightly higher crack initiation stress than those from the direction parallel, but AE has an opposite result, see Figure 4-10(b) for reference.

(5) Indicated by UCS testing (except G20) and AE results, shown in Figure 4-11, samples collected from the starting part of the core boreholes exhibit slightly higher crack initiation stress than those from the end part.

(6) Similar to UCS, it can be found from Figure 4-12 that, among the four combinations according to sample direction and distance, the group of samples collected near the deposition hole wall in the direction perpendicular to major principal stress has the highest average CIS and the other three groups have very near average CIS values. (7) As shown in Figure 4-13, the coefficients of variation are less than 0.25 for CIS determined by UCS testing and about 0.10 for CIS determined by AE, which are comparable to those for Äspö HRL. As a whole, the scatter in CIS is small. Compared according to sample´ distance, the samples collected near the deposition hole wall have slightly higher variation coefficient of CIS by UCS testing, but relatively lower variation coefficient of CIS by AE. The samples from the direction perpendicular to major principal stress have slightly lower variation coefficient of CIS by UCS testing but relatively higher variation coefficient of CIS by AE than those from parallel direction.

4.3.3 Crack volumetric strain

Figure 4-14 shows the relationship between the crack volumetric strain and the axial stress, and Figure 4-15 shows the comparison with results from ASPE. From these diagrams, CIS and corresponding crack volumetric strain can be determined. The results of crack volumetric strain at CIS and total volumetric strain at CDS are listed in Table 4-4.

Table 4-4. Crack volumetric strain at CIS and CDS

Experiment	Rock type	Sample No	ε_{vc} at CIS	ε_{v} at CDS
CRT	Greenstone	G17-113-1	0.000249	0.00072
		G17-113-2	0.000345	0.00085
		G18-113-1	0.000255	0.00078
		G18-113-2	0.000294	0.00067
		G20-113-1	0.000189	0.00075
		G20-113-2	0.000279	0.00075
		G21-113-1	0.000216	0.00080
		G21-113-2	0.000119	0.00061
		Mean	0.000243	0.000741
		Standard deviation	0.000069	0.000076
	Äspö diorite	G19-113-1	0.000271	0.00096
		G19-113-2	0.000330	0.00087
		G22-113-1	0.000243	0.00092
		G22-113-2	0.000161	0.00080
		Mean	0.000251	0.000888
		Standard deviation	0.000070	0.000067
ASPE		U499	0.000113	
		U538	0.000112	
		U543	0.000124	
		U626	0.000201	
		U737	0.000122	
		Mean	0.000134	
		Standard deviation	0.000037	

Figure 4-16 and Figure 4-17 are the histograms showing the comparison of crack volumetric strain at CIS according to sampled direction and distance. Figure 4-18 shows the comparison of crack volumetric at CIS with that from APSE. Figure 4-19 and Figure4-20 show the average values and variation coefficient of crack volumetric strain at CIS for different combinations of samples, respectively.

Based on these results, the following findings can be made:

(1) As shown in Table 4-4, Figure 4-15 and Figure 4-18, compared with data from ASPE, Äspö diorite in CRT deposition hole has the similar curve pattern of crack volumetric strain versus axial stress and comparable but somewhat larger crack volumetric strain at CIS, this might be attributed to the lower strength of CRT rock.

(2) As can be seen from Figure 4-16 and Figure 4-19, samples from the direction perpendicular to major principal stress unanimously have slightly higher crack volumetric strain at CIS than those from the parallel direction. For the 6 samples collected near the deposition hole wall, the average crack volumetric strain at CIS for the three samples from the direction perpendicular to major principal stress (marked as start-perp combination in the Figure 4-19) is higher than that for samples from the parallel direction (marked as start-para combination in the Figure4-19) by about 0.00004(about 18%). For the other 6 samples collected about 1.5m away from the deposition hole wall, the average crack volumetric strain at CIS for the three samples from the direction perpendicular to major principal stress(marked as end-perp combination in the Figure 4-19) is higher than that for samples from the parallel direction (marked as end-para combination in the Figure4-19) by 0.00013.

(3) Compared according to the distance to the deposition hole wall, as shown in Figure 4-17, in the direction perpendicular to major principal stress, samples collected near the deposition hole wall have lower crack volumetric strain than those from the end part.

(4) It can be seen that the variation coefficient of crack volumetric strain at CIS is smaller for samples collected in the direction perpendicular to major principal stress and those collected near the deposition hole wall.

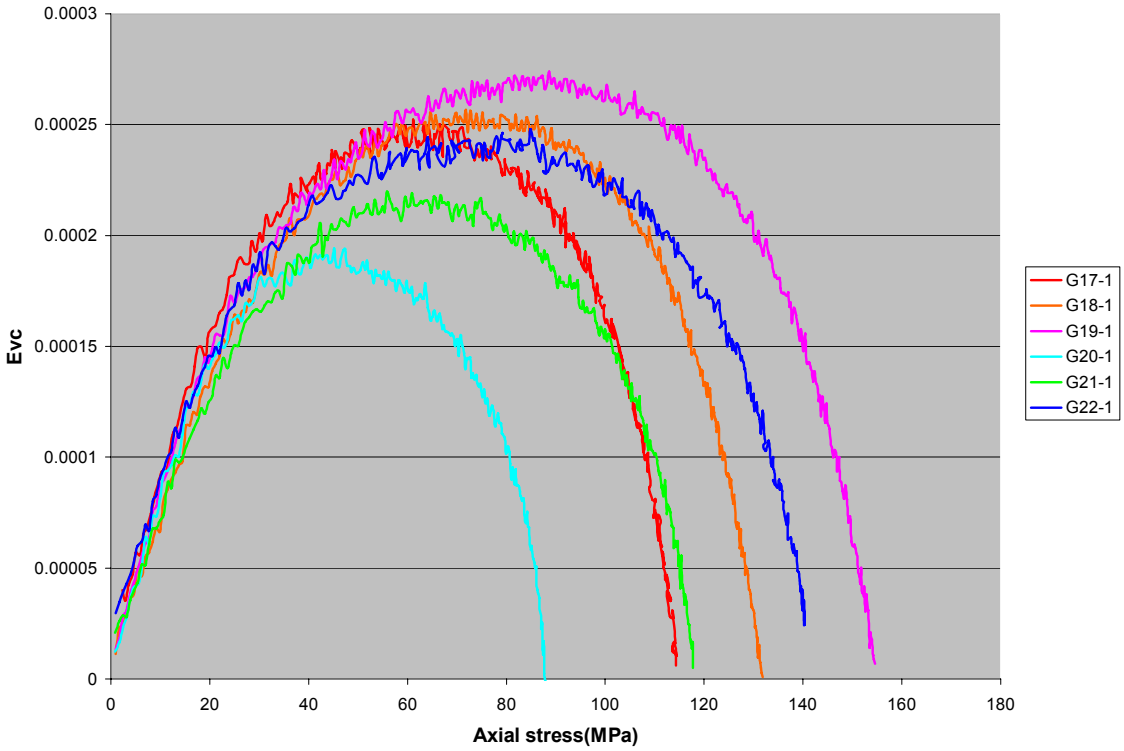

(a) Samples collected near the deposition hole wall

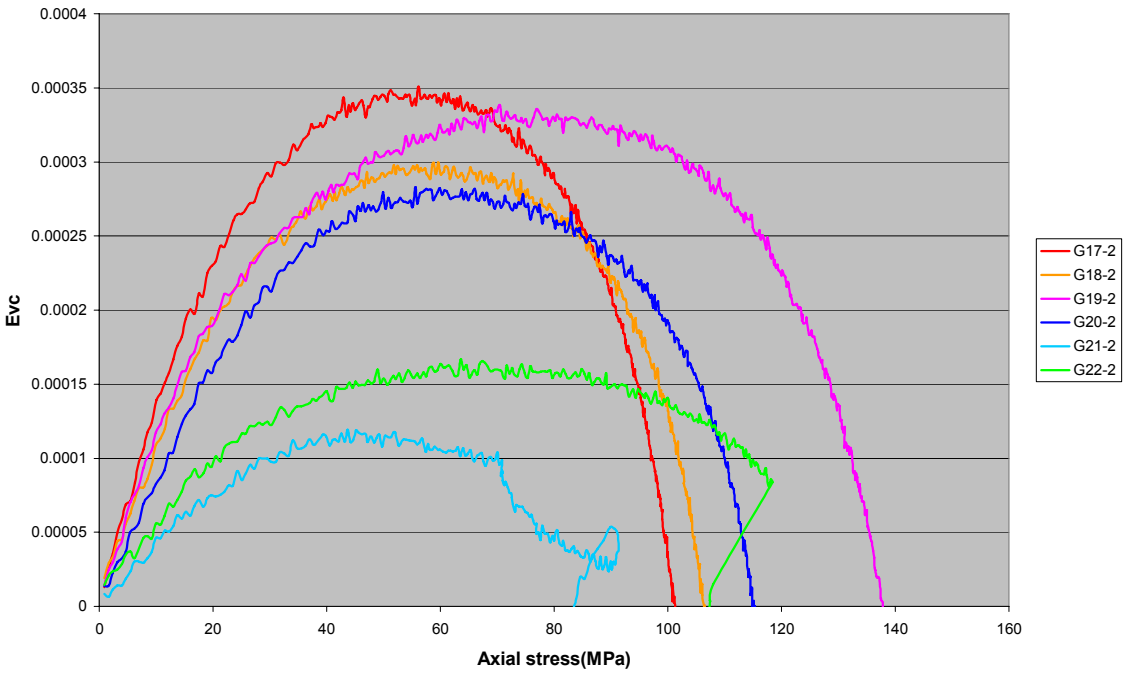

(b) Samples collected about 1.5m away from the deposition hole wall

Figure 4-14. *Relationship curves between axial stress and crack volumetric strain.*

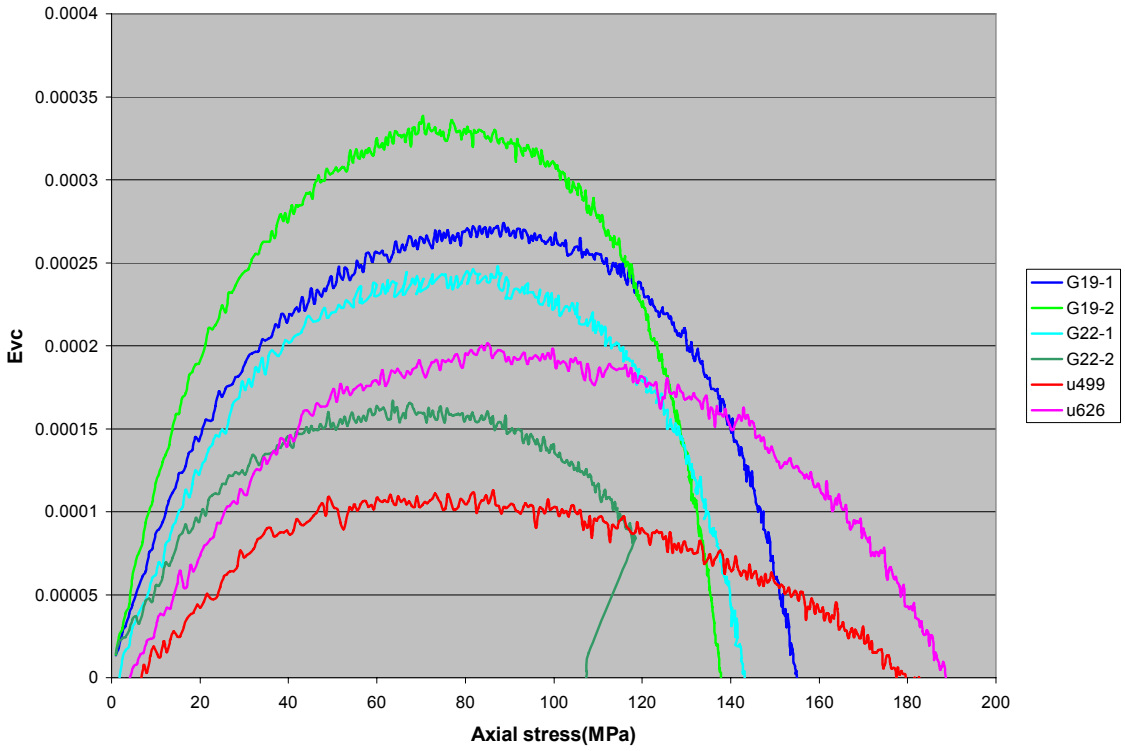

Figure 4-15. *Crack volumetric strain versus axial stress:comparison with data from APSE.*

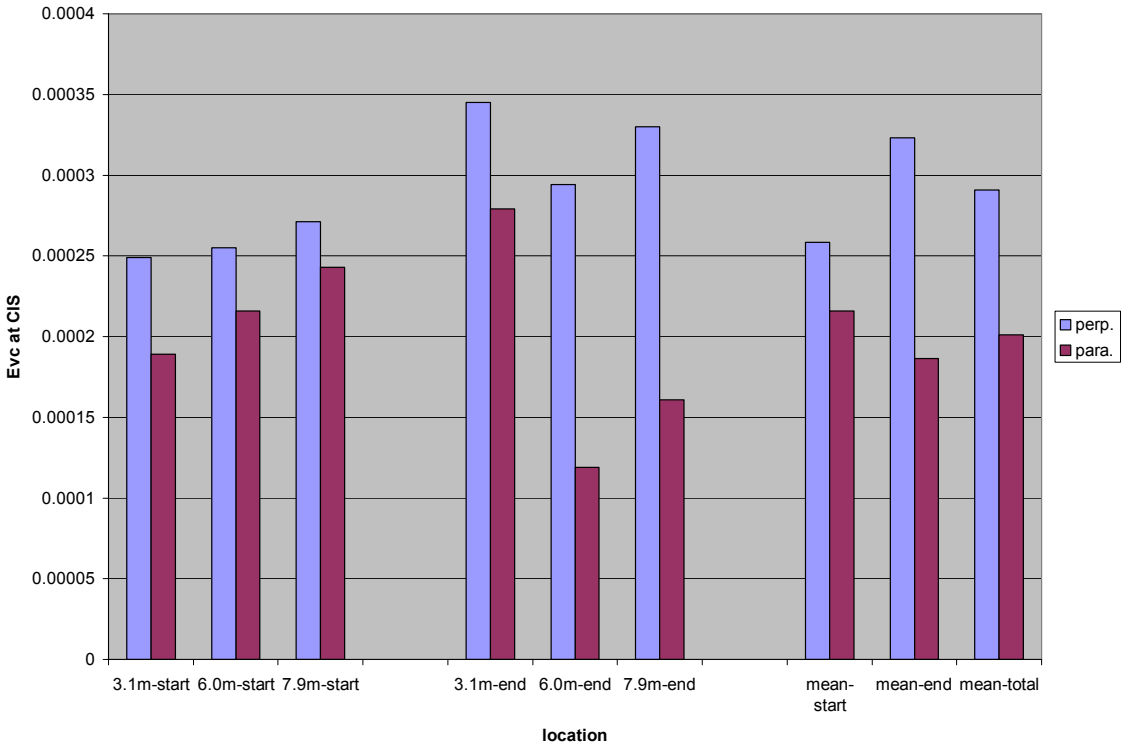

Figure 4-16. *Comparison of crack volumetric strain at CIS between samples from the direction parallel and perpendicular to major principal stress.*

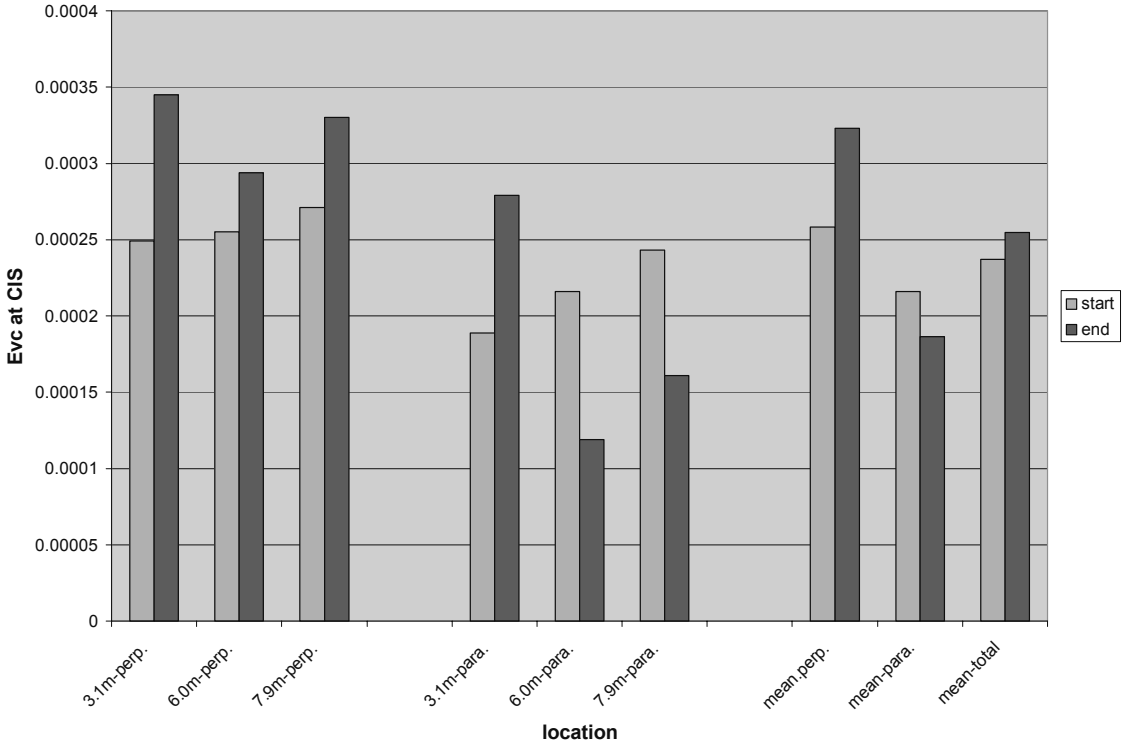

Figure 4-17. *Comparison of crack volumetric strain at CIS according to the distance to the deposition hole wall.*

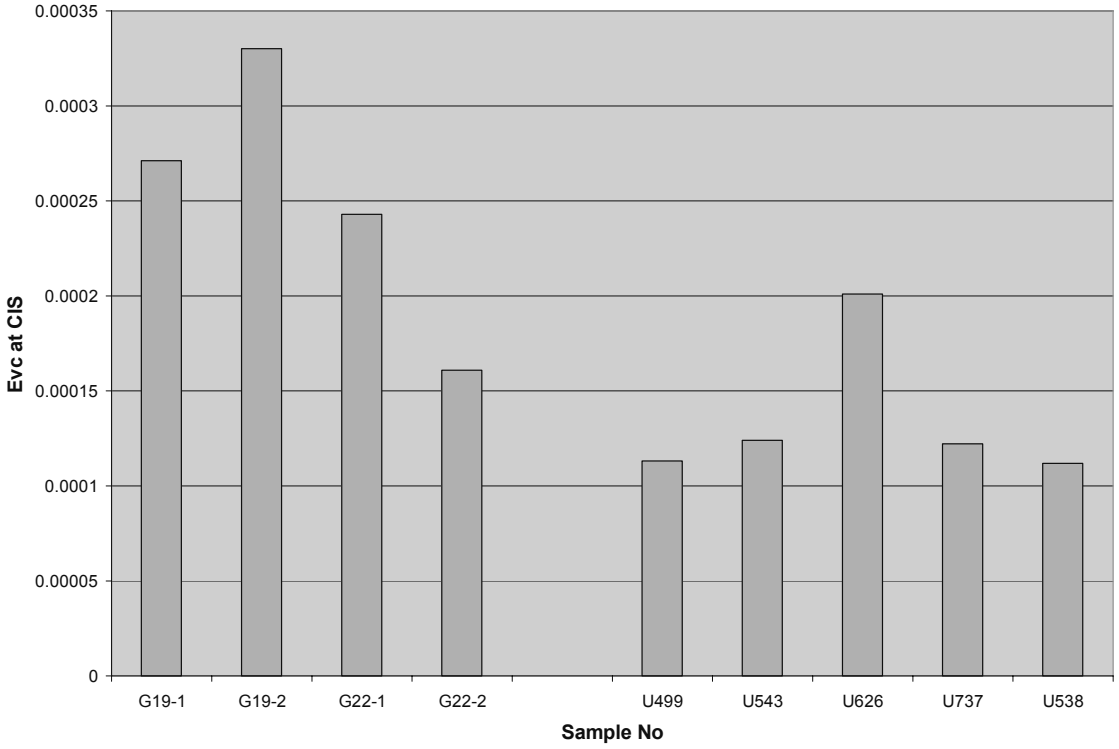

Figure 4-18. *crack volumetric strain at CIS: comparison with ASPE.*

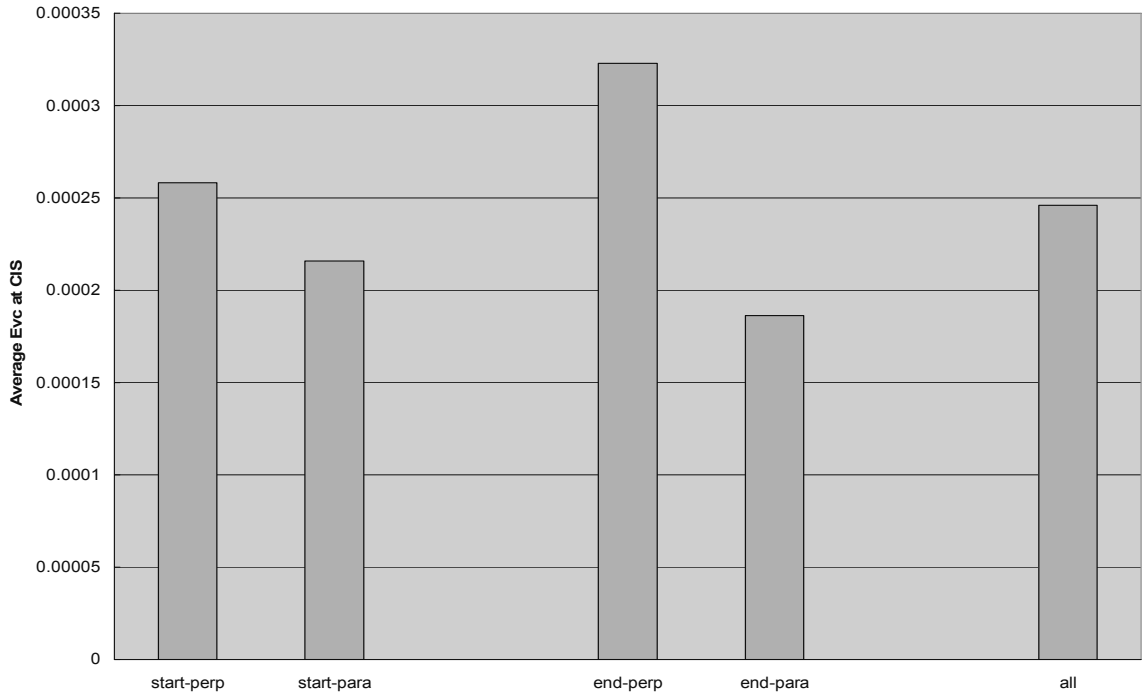

Figure 4-19. *The mean values of crack volumetric strain at CIS for different combination of direction and distance and comparison with that for all samples.*

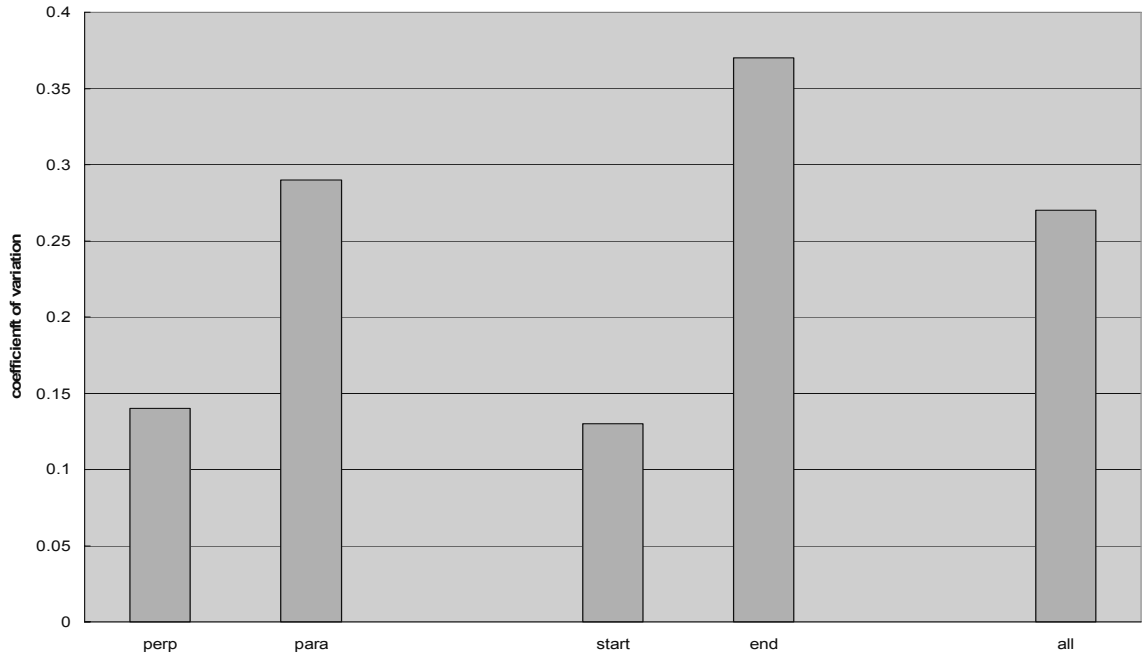

Figure 4-20. *Coefficient of variation of crack volumetric strain at CIS for different combination of samples and comparison with that for all samples.*

4.3.4 Damage analysis from UCS testing

The results from UCS testing, including UCS and Young´s modulus, crack initiation stress and crack damage stress, and crack volumetric strain, have been complied and analyzed respectively.

By comparing testing results of samples from different direction, it has been found that the UCS, Young´s modulus, crack initiation stress (determined from $\varepsilon_{vc} - \sigma$ curves) and crack damage stress in the direction perpendicular to major principal stress are higher than those in the direction parallel to major principal stress. By comparing testing results of samples from different distance to the deposition hole wall, it has been found that, except in G20, the UCS, Young´s modulus and crack initiation stress at the starting part of the core boreholes are higher than those at the end part. By dividing the 12 samples into 4 combinations according to direction and distance, it has been found the combination of perpendicular direction with starting part has the highest average values of UCS and crack initiation stress, whereas the combination of perpendicular direction with end part has the lowest average Young´s modulus. The coefficients of variation of UCS, Young´s modulus and crack initiation stress have no unified variation tendency with sampled direction or distance. Theoretically, the rock where perpendicular-start combination samples were collected should have been maximum loaded due to excavation and heating. But from the above-mentioned comparisons, there is no evidence of damage by UCS, E, CIS and CDS in this combination. Therefore, it can be inferred that the surrounding rock of the CRT deposition hole had no obvious damage.

Analysis of crack volumetric strain indicated samples from the direction perpendicular to major principal stress unanimously have slightly higher crack volumetric strain at CIS than those from the parallel direction. In the direction perpendicular to major principal stress, samples collected near the deposition hole wall have lower crack volumetric strain than those from the end part.

Figure 4-20 is the normalized results by taking the average values of UCS, E, CIS and ε_{vc} at CIS of perpendicular-start combination as 1. It is clear in Figure 4-20 that samples belonging to the perpendicular-start combination have the highest average values of UCS and CIS, and similar high value of Young´s modulus as para-start and para-end combinations. For the six samples from the starting part but different direction at the three depths, noting that the six samples have almost the same Young´s modulus and the three samples from the direction perpendicular to major principal stress have higher UCS than the other three from the parallel direction, it seems reasonable to attribute this slightly higher value of crack volumetric strain to some micro-fracturing in the corresponding rock due to excavation and heating during the CRT experiment. But the micro-fracturing occurred only to a small extent, if it did exist. For the six samples from the different part of the core boreholes in the direction perpendicular to the major principal stress, the relatively great difference in average crack volumetric strain should be related to the geological difference and might be prescribed to the lower Young´s modulus of the samples from the ending part of the core boreholes. The possible damage in the form of micro-fracturing due to excavation and heating was seemingly masked.

In summary, judged from UCS, Young's modulus, CIS and CDS, the surrounding rock of the CRT deposition hole had not been damaged during the CRT. Crack volumetric strain data show that micro-fracturing might have occurred, but only to a small extent.

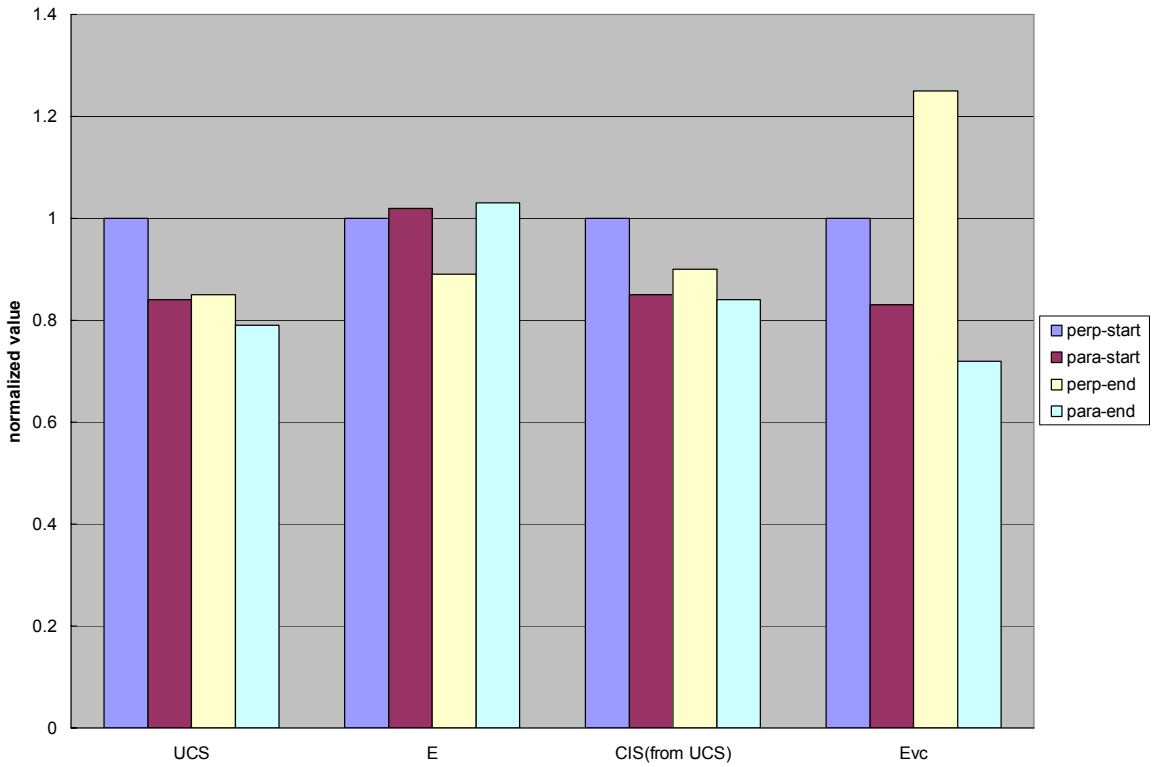

Figure 4-21. *Normalized values of average UCS,E,CIS and Evc for different combinations.*

5 Numerical simulation

5.1 Software

The thermal and thermal-mechanical modelling computations in this study were performed using Itasca´s FLAC500 software (Itasca 2005). FLAC500 is a two-dimensional explicit finite-difference program for engineering and mechanics computation. Ten material models, including several describing highly non-linear, irreversible response, are built in FLAC500, and new constitutive models can be added via the FISH programming language. Plane-strain, plane-stress and axisymmetric geometry modes can be computed. Thermal and thermal coupling to mechanical stress and pore pressure are optionally available. Thermal-mechanical coupling in FLAC is one-way: temperature change may induce a mechanical stress, however, mechanical changes do not result in temperature change.

Most practical engineering problems are strictly three-dimensional, but in some cases, it can be simplified as a two-dimensional problem and problem solution becomes much moreconvenient and time-saving. In this study, it is reasonable to assume it as a vertically thermally axisymmetric mode and in the area near the middle height of the canister as a coupled thermal-mechanical plane-stress mode. Therefore, by comparing with some measured results, it provided an opportunity to test the capability of FLAC2D to calculate the temperature, stress and possible damage when applied to such a case. Elastic mechanical and isotropic thermal conductive models were used for this study.

5.2 Model and parameters

5.2.1 Model geometry

The geometries for axisymmetric thermal and for plane mechanical-thermal coupling analyses are as Figure 5-1. The axisymmetric geometry is 20m wide and 25m high with 6750 elements. The plane thermal- mechanical coupling geometry is a quarter circle generated by FLAC FISH grid generation tool with an inner radius of 0.875m and an outer boundary of 20m, and the total element number is about 2000.

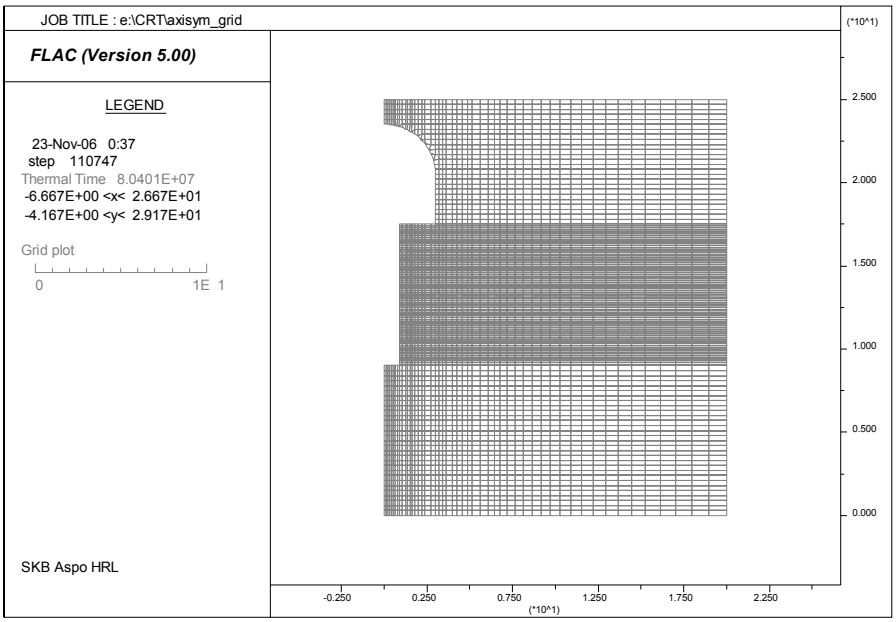

(a) axisymmetric thermal analysis geometry

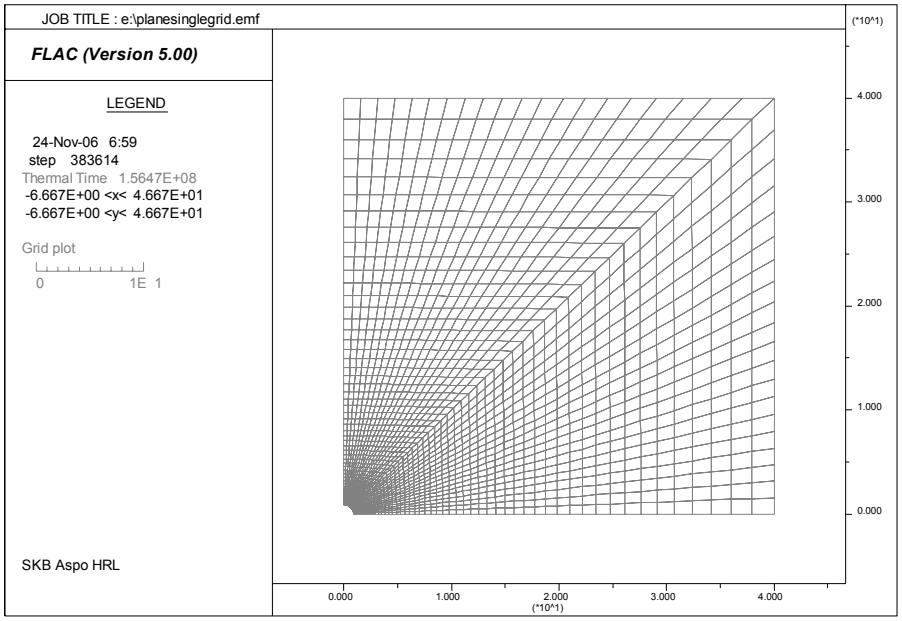

(b) Plane thermal-mechanical analysis geometry

Figure 5-1. *Sketch of the model geometry.*

5.2.2 Material properties

Density and mechanical propeties (Young´s modulus and Poisson´s ration) needed for this modelling were obtained from the UCS testing as described in the previous chapter. The mean values for each rock type were used for basic case modelling and are listed in Table 5-1.

Table 5-1. Rock properties used for basic case modelling

Rock type	Density (kg/m3)	Young´s modulus(GPa)	Poisson´s ratio
Greenstone	2824	58.2	0.32
Äspö diorite	2738	64.4	0.31

The isotropic heat conductive model was adopted for the heat transmission within the rock volume in this study, hence thermal properties of the rock needed for modelling included conductivity, specific heat and linear expansion coefficient. No such measurement had been made specifically for CRT rock volume. The thermal properties were obtained with reference to such data for prototype repository and ASPE and are listed in Table 5-2.

Table 5-2. Thermal properties for basic case modelling

Rock type	Conductivity, K (W/m,K)	Specific heat, Cv (J/kg,K)	Linear exp. coeff. ($1/^0C$)
Greenstone Äspö diorite	2.6	778	$7e^{-6}$

5.2.3 Thermal load and thermal flux

The heating process and heat power of the canisters were described in 3.3 and used for the modelling.

For vertical axisymmetric thermal modelling in CRT deposition hole, the thermal flux was assumed to be the heat power divided by the hole surface area in the length of the canister and the hole wall above and below the canister section were set a very small flux.

For horizontal thermal-mechanical coupling modelling, the thermal flux was obtained by treating the canister as a compound line source, which means that the 0.2125m end-sections at the top and bottom of the canister had a heat flux of 3.15 times that at the other 4.41m part of the canister height (Harald Hökmark, 2003).

5.2.4 Initial and boundary conditions

The initial temperature in the rock and the temperature in the tunnel were set as 150C. No rock stress measurement in the CRT rock volume was performed. Referring to rock stresses in TASQ and the equations of in-situ stress for Äspö given by Hossin Hakami,2003, rock initial stresses listed in Table 5-3 were used for the basic case modelling.

Table 5-3. Initial stresses for basic case modelling

Principal stress	Magnitude (MPa)	Trend/dip (^{0})
σ_1	30	310/0
σ_2	11	/90
σ_3	10	40/0

Mechanically, all the free boundaries were prescribed to be zero force, whereas the other embedment boundaries were not allowed to move in the normal direction to the surface.

Thermally, the free surfaces to the tunnel were treated as convection boundary, with the convection heat transfer coefficient prescribed to 10W/ (m^2K). The symmetric planes were prescribed to be adiabatic. The outer boundaries were temperature-fixed (as initial temperature 15^{o}C).

The total pressure (swelling and water pressure) acting on the hole wall varied temporally and spatially. For the base case, it was assumed to be 3MPa and act from the time when CRT heat power was raised from 1700W to 2600W (about 100days after start, see Figure3-6).

6 Results

6.1 Temperature

Figure 5-2 through Figure 5-5 are diagrams showing the variations of calculated temperature with time at different depths calculated from axisymmetric thermal analysis. Figure 5-6 and Figure 5-7 are temperature results calculated from horizontal thermal-mechanical coupling analyses of single hole and double hole (CRT and TBT), respectively.

From these figures, the following conclusions can be drawn:

(1) Temperatures at different depths and different distance from the heating hole wall can be reasonably calculated by axisymmetric thermal analysis.

(2) The calculated temperatures at different depths from axisymmetric thermal analyses by FLAC500 generally well match the measured results before the TBT started heating. The temperature of hole wall in the middle of the canister is slightly higher than measured and lower than measured at the top and bottom of the canister; this can be partly attributed to the neglect of the heat dissipation from the bottom and top area of the canister.

(3) The temperatures calculated from horizontal plane analysis basically agree with the measured results at the middle height of the canister before about 100days, but much higher than measured results at the bottom and top depths of the canister for all the time and at the middle height of the canister after 100days. The difference is even higher after superimposition of the influence from TBT heating.

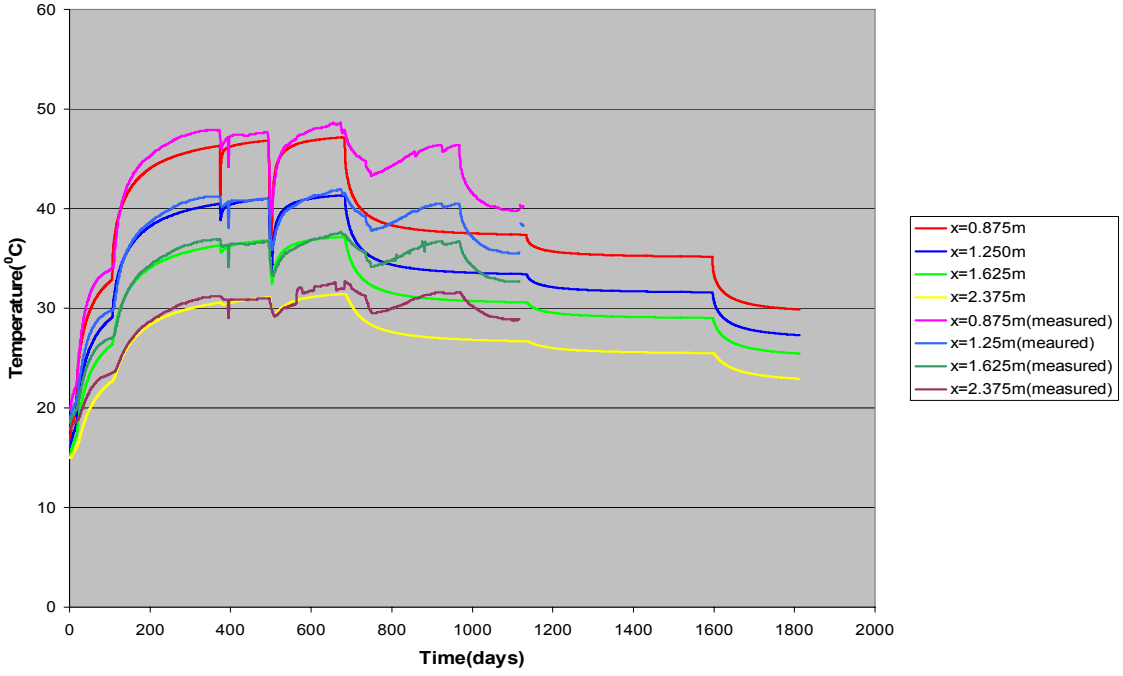

Figure 5-2. *Variation of calculated and measured temperature with time at depth 3.1m from axisymmetric analysis*

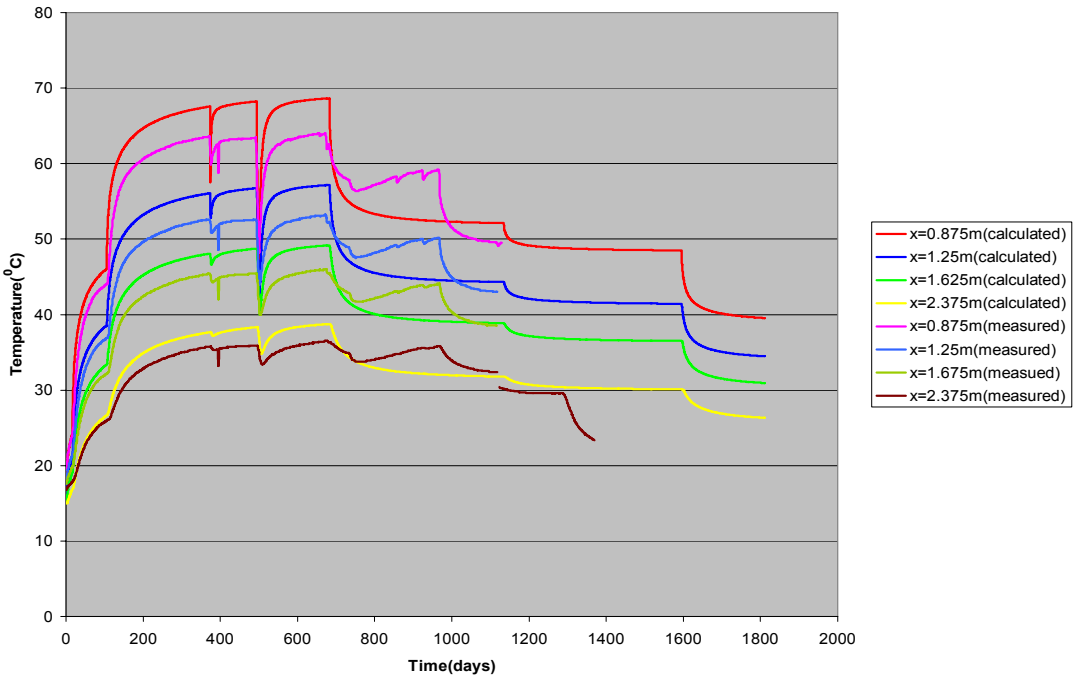

Figure 5-3. *Variation of calculated and measured temperature with time at depth 5.5m from axisymmetric analysis.*

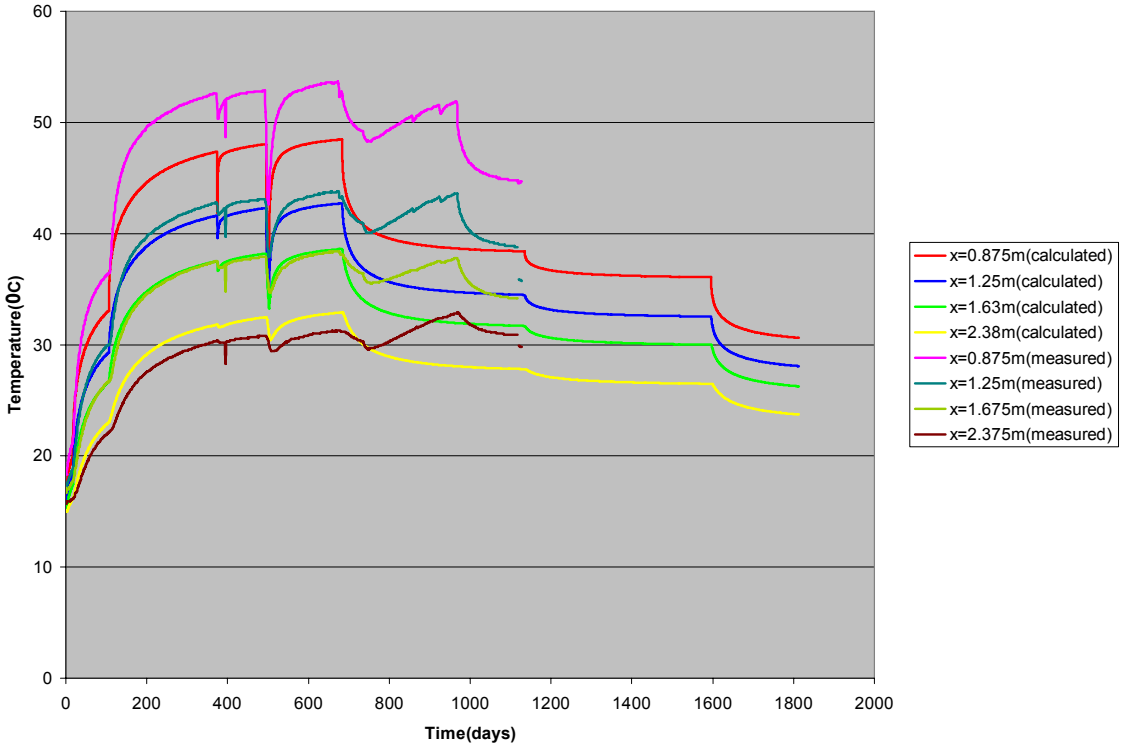

Figure 5-4. *Variation of calculated and measured temperature with time at depth 7.9m from axisymmetric analysis.*

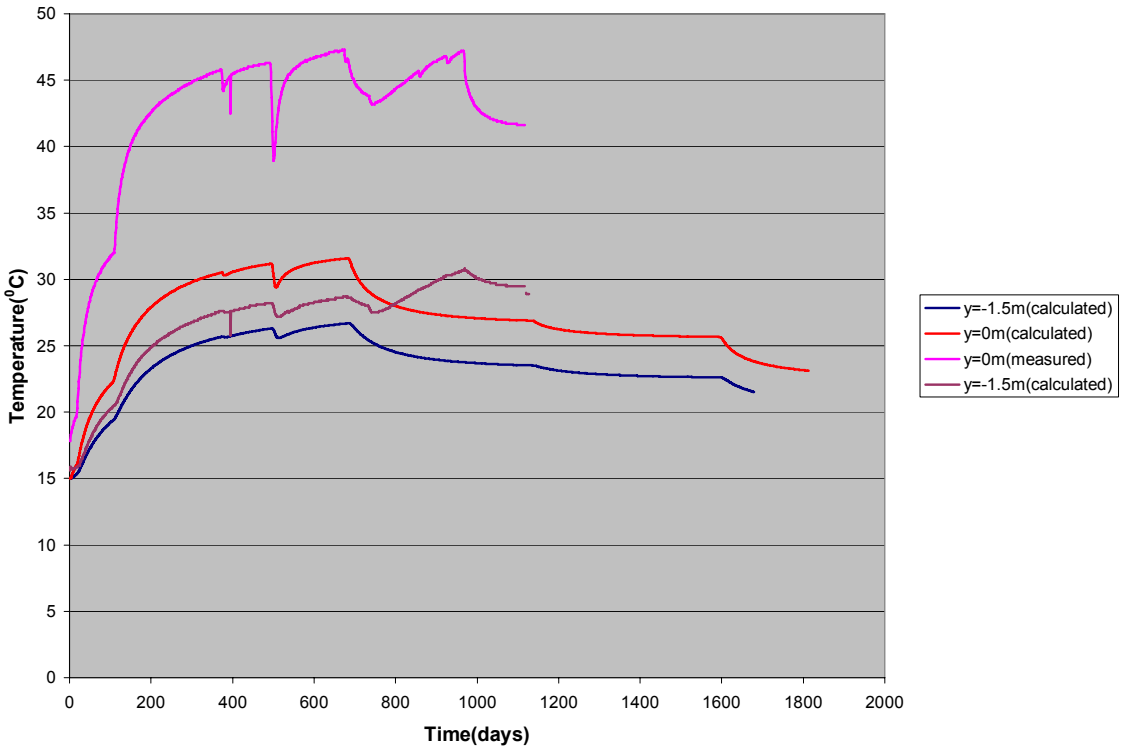

Figure 5-5. *Variation of calculated and measured temperature with time in the center under the hole from axisymmetric analysis.*

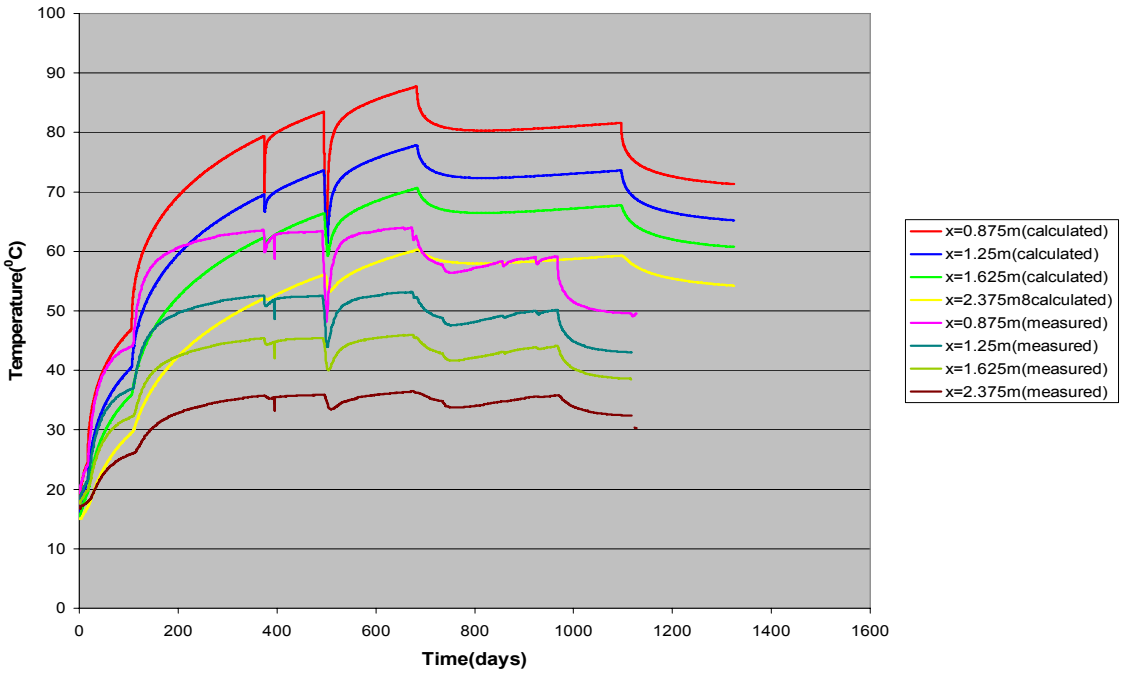

Figure 5-6. *Variation of calculated and measured (at 5.5m) temperaturewith time from plane analysis of single hole.*

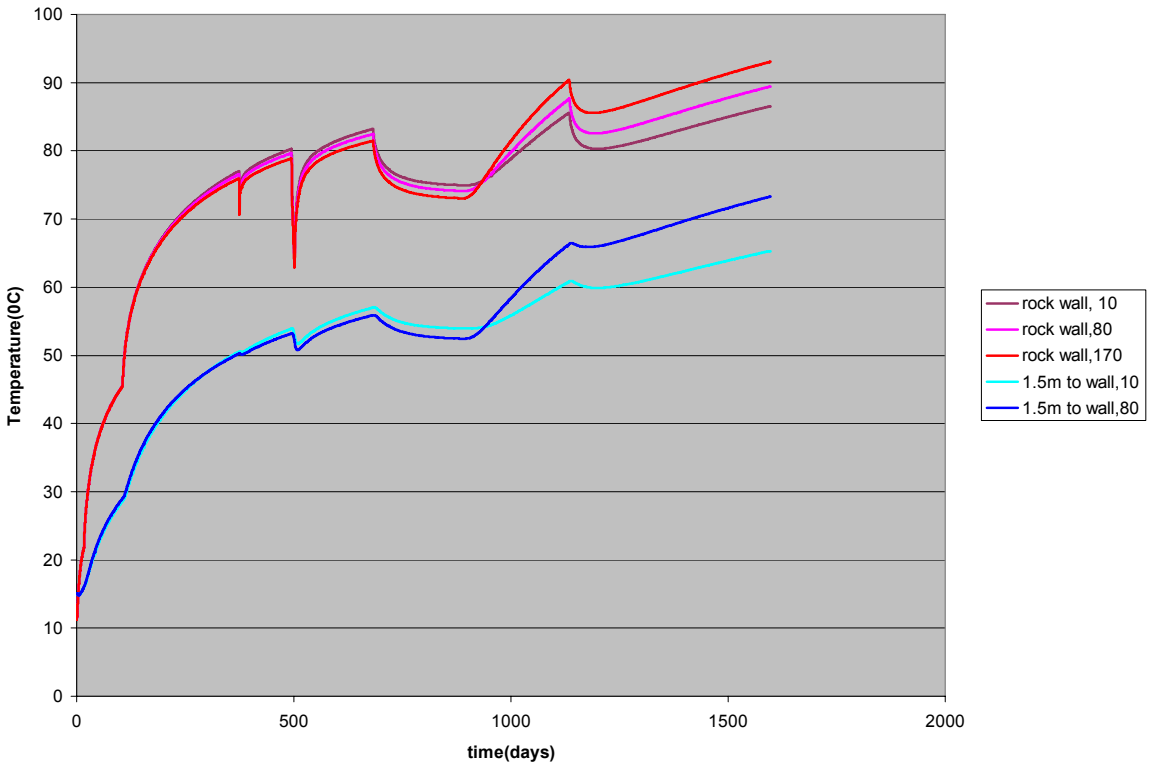

Figure 5-7. *Variation of calculated temperature with time from plane analysis of double holes(CRT and TBT).*

(for angle in the legend, refer to Figure 3-7)

6.2 Stress

Figure 5-8 shows the calculated major principal stress variation with time at the centre of zone (1, 1) and zone(1,40) from plane thermal-mechanical coupling analysis. From the calculation, the maximum principal stress was located in Zone (1, 1) and the value was about 120MPa at the time when the highest heat power ended. Figure 5-9 are variation of calculated principal stress with time for zones parallel and perpendicular to the tunnel axis at about 30cm away from the deposition hole wall, where stress changes were measured at all the stages during the experiment period. The calculated stress increase change at these points was 5-10MPa after excavation and 40-50MPa during heating stage. The measured maximum stress increase was 22MPa during drilling stages and 82MPa during heating stage. The measured results (uncompensated for temperature) exhibited large scatter and the difference between calculated and measured is obvious.

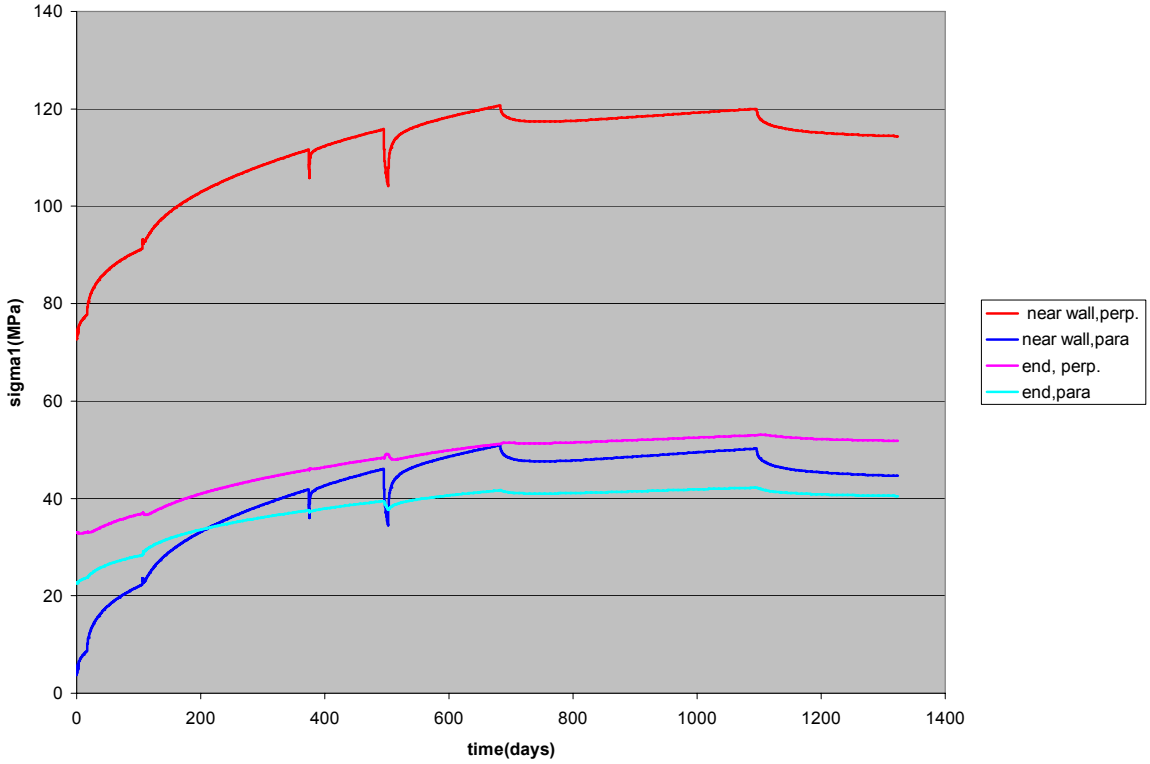

Figure 5.-8. *Major principal stress near and 1.5m away from hole wallalong direction parallel and perpendicular to σ1.*

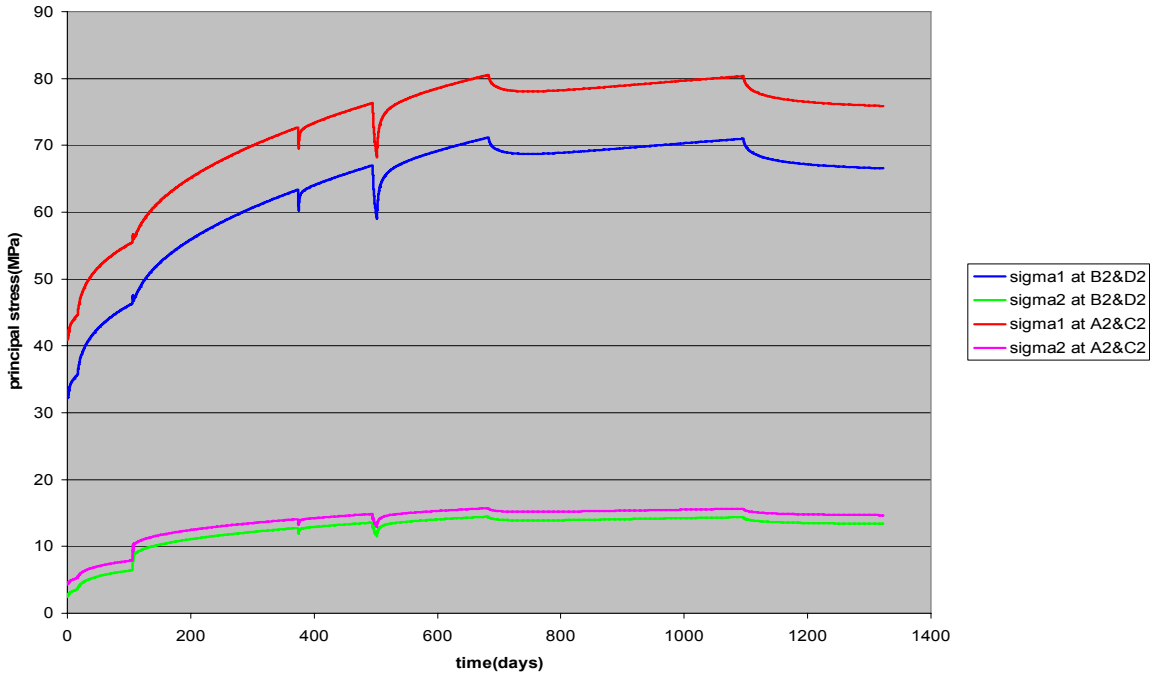

Figure 5-9. *Calculated major and minor principal stress at the stress measurement points.*

(Refer to Figure 3-2 for location A2,B2,C2,D2)

6.3 Approximate damage analysis

The calculated temperature from previous plane thermal-mechanical analysis is about 15^0C higher than measured and might overestimate the heat induced stress. To get a more reasonable temperature from the numeric modelling for the possible damage analysis, the measured temperatures at rock wall of the deposition hole were simplified as stepwise rise and used as temperature boundary. Based on the measured rock wall temperature at three depths, temperatures in the rock at corresponding depths were obtained and stresses were accordingly calculated.

As stated in 3.5 from measured results, the maximum loaded part in the rock reached its temperature climax when the CRT heat power was changed from 2600W to 1600W at about day 683. Therefore, the calculation for damage analysis was conducted to a time period of 683 days.

Figure 5-10 to Figure 5-12 show the calculated temperature variation with time. It can be found that the results for the inner part which is of interest to damage analysis are quite consistent with measured results, for the outer part, the calculated results are still higher than measured results, but the difference is much smaller compared with previous analysis.

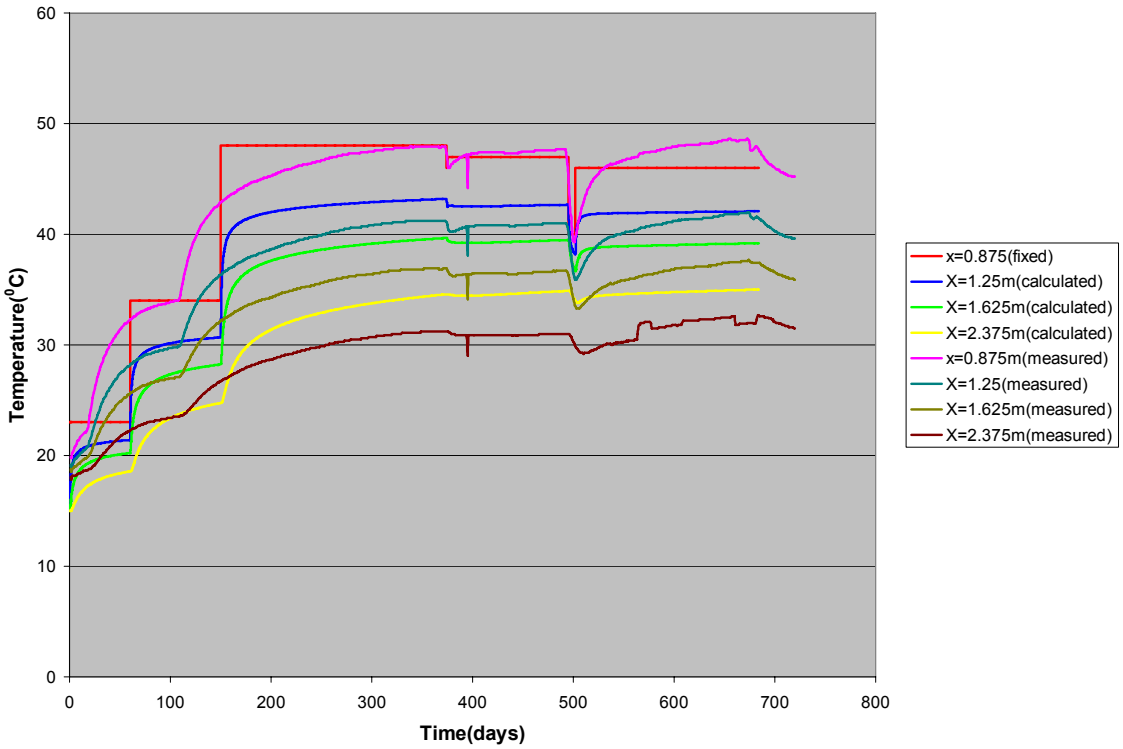

Figure 5-10. *Variation of calculated temperature with time at depth 3.1m from plane analysis by fixing the wall temperature and its comparison with measured results.*

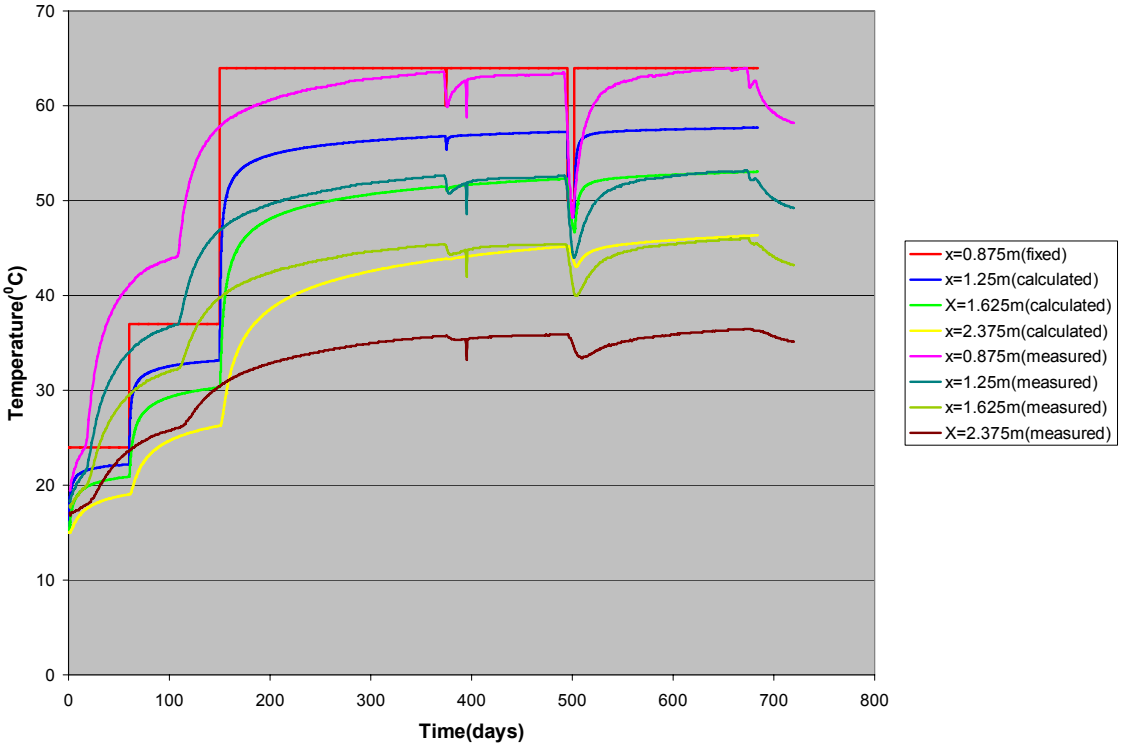

Figure 5-11. *Variation of calculated temperature with time at depth 5.5m from plane analysis by fixing the wall temperature and its comparison with measured results.*

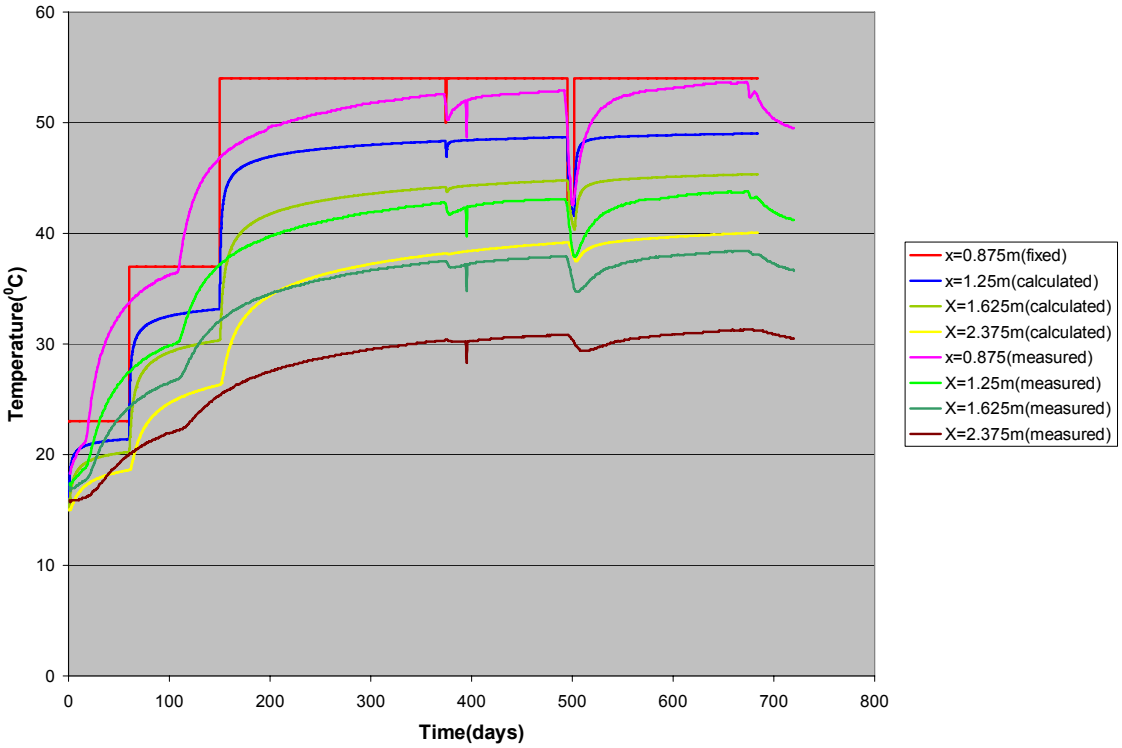

Figure 5-12. *Variation of calculated temperature with time at depth 7.9m from plane analysis by fixing the wall temperature and its comparison with measured results.*

Figure 5-13 through Figure 5-15 show the variation of major principal stress (including excavation and heat induced stress) with time at the sampled points at three depths. Some values of CIS were also presented. It can be seen that the major principal stress at points along the direction perpendicular σ1 is much higher than that parallel to σ1.

The calculated major principal stress (tangential stress) after excavation was about 76MPa near the hole wall in the perpendicular direction and was increased to the maximum values of about 95MPa, 105MPa and 100MPa on day 683 during the heating stage at depth 3.1m, 5.5m and 7.9m respectively. The minor principal stress (radial stress) on the hole wall was 0 after excavation and was about 3MPa due to the bentonite swelling pressure. Compared with the crack initiation stresses discussed in the previous chapter, the three samples, numbered G17-113-1, G18-113-1 and G19-113-1, with the crack initiation stress of 65MPa, 75MPa and 80MPa, and crack damage stress of 100MPa, 115MPa and 140MPa, respectively, should have be loaded to stress over or near their crack initiation stresses after excavation and near to (G17-113-1, G18-113-1) or about 30MPa lower(G19-113-1) than their crack damage stresses. Therefore, it could be inferred in this model that the rock where these samples were collected could have been damaged to a great extent if the influence of minor principal stress on the crack initiation stress could be neglected.

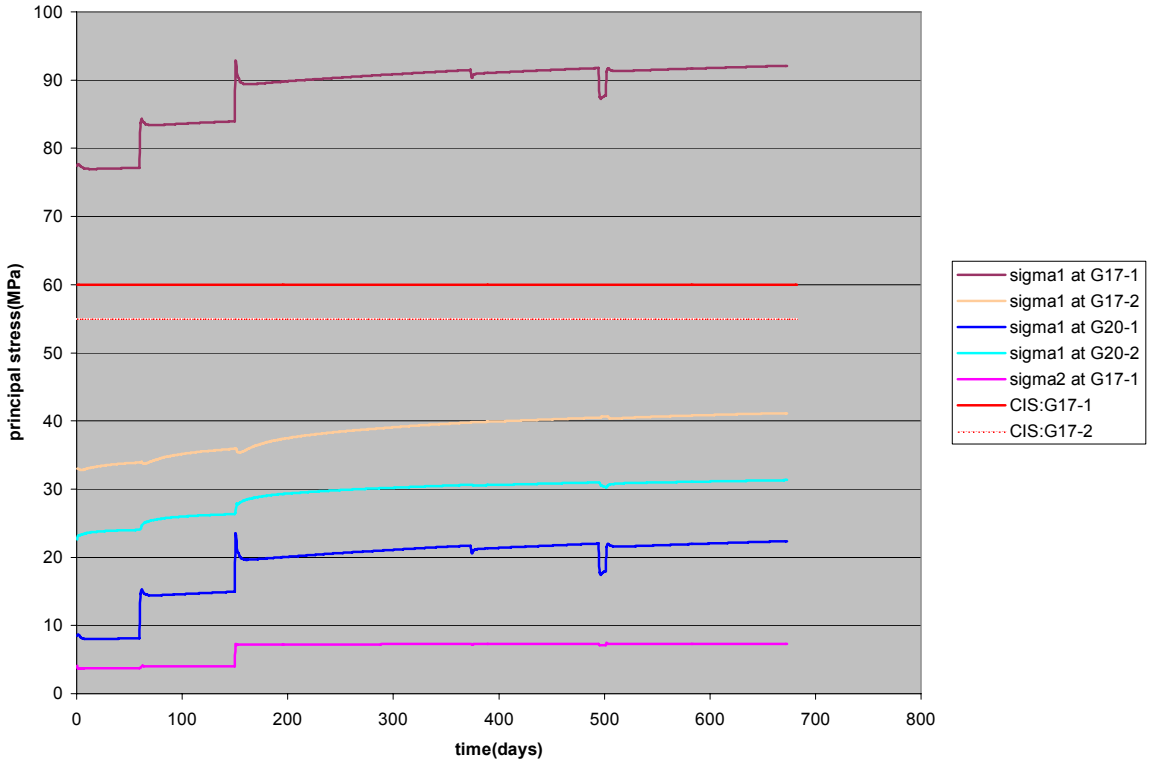

Figure 5-13. *Variation of calculated major principal stress near the deposition hole wall at depth 3.1m.*

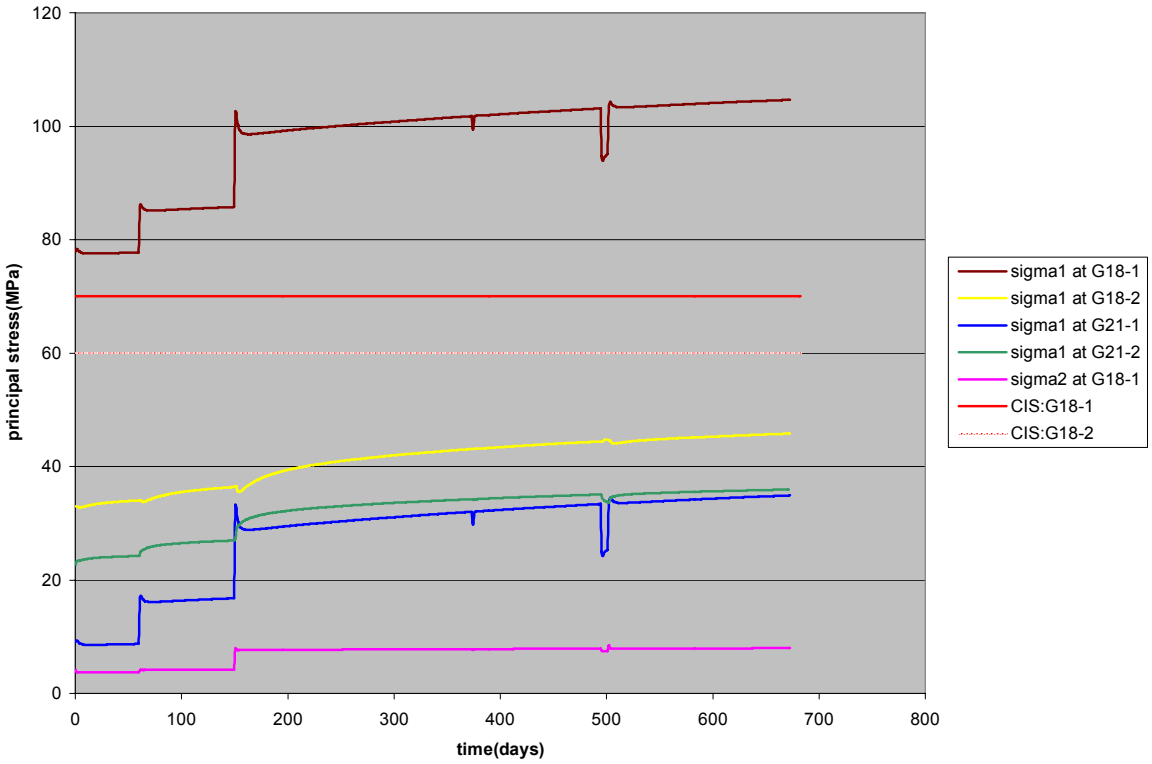

Figure 5-14. *Variation of calculated major principal stress near the deposition hole wall at depth 5.5m.*

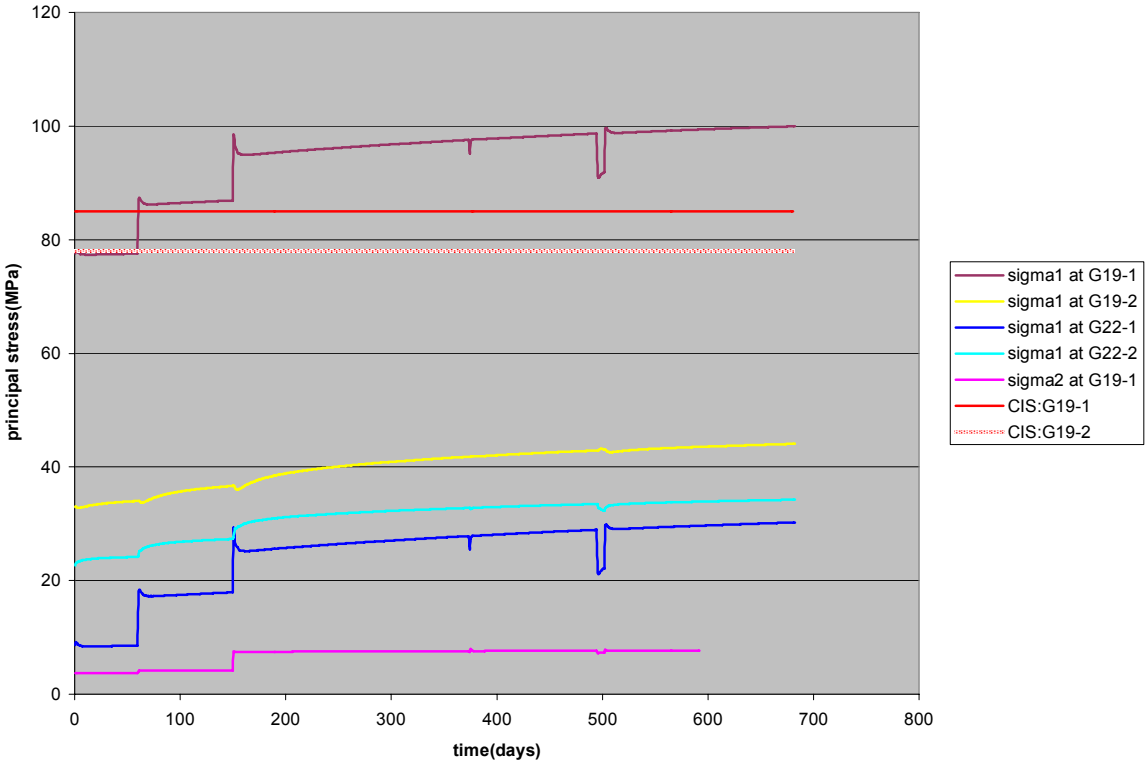

Figure 5-15. *Variation of calculated major principal stress near the deposition hole wall at depth 7.9m*

The major principal stresses at points where all the other samples were collected were less than 45MPa. Therefore, all the other samples had not experienced the stress greater than their crack initiation stress and should have not been damaged.

There were some uncertainties related to the modelling. For this reason, sensitivity analysis at depth 5.5m was conducted. As far as 2D is concerned, the main uncertainties in this modelling and the varied values are listed in Table 5-3. The variation of calculated principal stress with time near the location of sample G17-1 for all cases were shown in Figure 5-17.

Table 5-3. Cases for sensitivity analysis

Case number	Changed parameter(s) from the base case
1	σ_1 =32 MPa, σ_2=17MPa
2	σ_1 =35 MPa
3	σ_1 =25 MPa
4	Thermal conductivity =2.92
5	Thermal expansion coefficient=8.4e-6
6	Swelling pressure=5MPa
7	Model size =40m

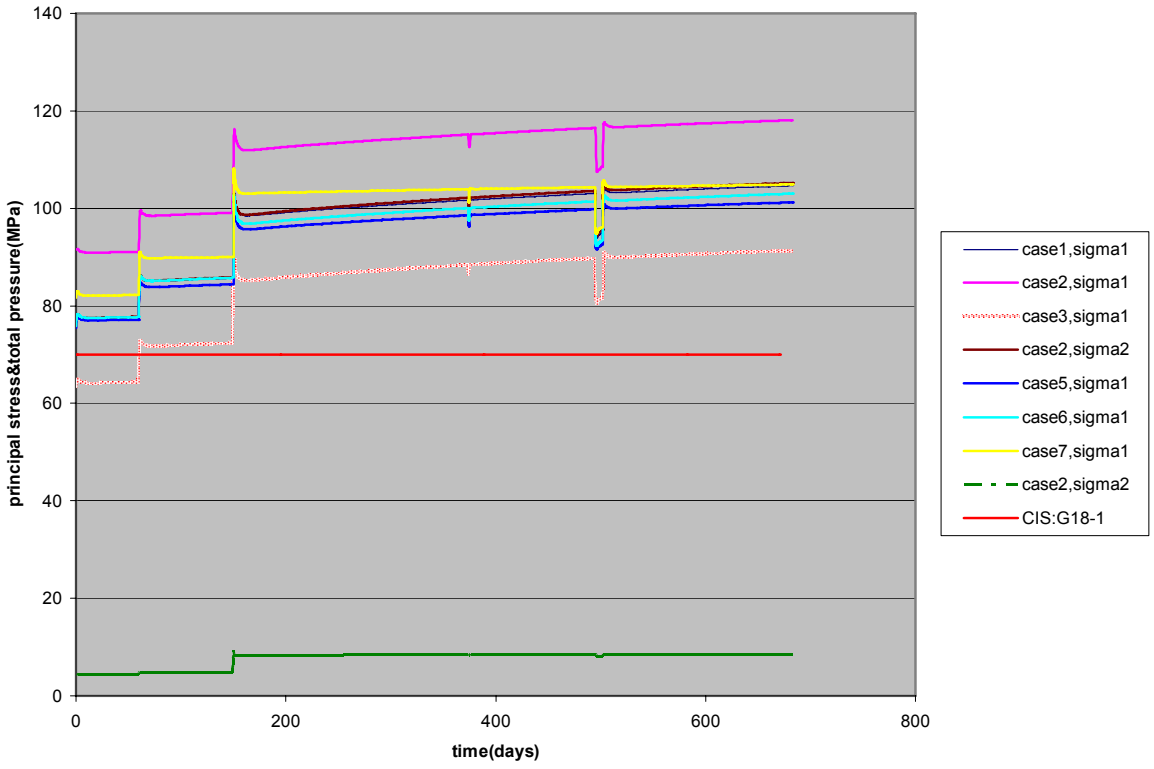

Figure 5-17. *variation of calculated principal stress with time for sensitivity analysis.*

It can be inferred from the sensitivity analysis that, by fixing the rock wall temperature, all the calculated cases have the major principal stress greater than crack initiation stress after heating to 683 days, and the same can be said even after excavation except case 3(in-situ major principal stress to be 25MPa). Therefore, main uncertainties in this study did not have much influence on the modelling analysis results.

7 Discussion

In this study, the possible heat-induced stress damage to the CRT deposition hole rock volume was investigated by uniaxial compression testing and two-dimensional numerical simulation.

Results from uniaxial compression testing performed on 12 core samples, taken from 6 sub-horizontal core boreholes drilled in DD0092G01, with different direction and different distance to the deposition hole wall, were analyzed and compared. Comparison was also made with some results from testing on cores for APSE. Judged from relatively higher values of crack volumetric strain at CIS, damage of small extent in the form of micro-fracturing probably occurred in the rock near the deposition hole wall in the direction perpendicular to the major principal stress after excavation of the deposition hole and during the later heating stage. There was no evidence of any damage by UCS, Young's modulus, CIS and CDS.

Axisymmetric thermal analysis generally generated temperature field quite consistent with measured results, whereas the temperature from plane analysis was much higher than measured. Much better results, especially for nearer part, were obtained by applying the measured rock wall temperature as a temperature boundary. The results of numerical modelling using such a heat boundary condition indicated that the tangential stresses in the rock near to the deposition hole wall in the direction perpendicular to the major principal stress at all three depths were higher or very near to the corresponding crack initiation stresses after excavation and near to the crack damage stress (G17-113-1, G18-113-1) during the heating stage. Sensitivity analysis shows the main uncertainties regarding the modelling did not change this result much. It could be inferred that the micro-fracturing in the damaged rock started after excavation and could have developed to a large and obvious extent during the heating stage, if the influence of minor principal stress on the crack initiation stress could be neglected.

The neighbouring TBT experiment, which started heating about 880 days later, at a time when the CRT heat power had been lowered from its maximum, had some influence on the temperature of the CRT deposition hole surrounding rock. But measured results indicate that the highest temperature was reached before TBT started. Therefore, for the purpose of damage analysis of the CRT surrounding rock, the influence from TBT was ignored.

The UCS testing and visual observation shows that the rock had not been damaged to the extent as conservatively predicated by numerical simulation (neglecting the influence of radial stress). This discrepancy is probably due to the existence of important influence of minor principal stress on crack formation and development. This was also observed in APSE. Damage in the form of micro-fractures in the rock near the wall in the direction perpendicular to major principal stress possibly occurred after excavation when the tangential stress reached the crack initiation stress and the radial stress was near zero. The further development was hindered due to the confining pressure arsing from the bentonite swelling in the hole during the heating stage, although the tangential stress was further increased and even to its crack damage stress.

The comparison in this study for UCS testing was conducted among samples taken from different locations after heating and not among samples of the same location taken prior to and after heating. The inherent spatial geological difference might have masked the damage to some extent.

The damage analysis by numeric simulation was conducted by 2D code. This might be a quite reasonable simplification for the area near the middle height of the hole. For the other part, the influence due to tunnel excavation or the end effect should have more important influence, which had not been taken into account in this study, thus the results for depth 7.9m is a rough estimate only. Also, as discussed above, neglect of the influence of radial stress on crack initiation stress might greatly overestimate the damage degree.

References

Carljohan Hardenby, 2002, Tunnel for the canister retrieval test:Geological mapping of tunnel and deposition holes. SKB International Progress Report IPR-02-49

Christer Svemar, 1999, Canister Retrieval Test:Test Plan Part 1 – Geotechnical characterisation, test installation and monitoring during saturation. SKB International Progress Report IPR-99-26

Peder Thorsager, 2002, Canister Retrieval Test Report on installation. SKB International Progress Report IPR-02-30

Reza Goudarzi, Lennart Bögesson, 2005, Canister Retrieval Test:Sensor data report (Period 001026-051101 Report No:11. SKB International Progress Report IPR-05-35

Harald Hokmark, Billy Falth, 2003, Thermal dimensioning of the deep repository-Influence of canister spacing, canister power, rock thermal properties and nearfield design on the maximum canister surface temperature. SKB Technical Report, TR-03-09

Hossin Hakami, 2003, Aspo site conditions: Rock Mechanics, updates 2003, SKB International Progress Report IPR-03-37

Acknowledgements

This study was conducted during the author´ three-month stay at SKB Äspö Hard Rock Laboratory as an IAEA fellow. The author is very grateful to IAEA, SKB and Äspö HLR for giving such a good opportunity.

Great thanks are given to the supervisor, Mr. Rolf Christiansson, for his careful arrangement in training programme and helpful academic instructions.

Thanks are also extended to Mr. Christer Andersson for his helpful academic discussions and suggestions, Mr. Carljohan Hardenby for his help in geological matters and Dr Eva Hakami for her support in numerical simulation.

Ms Therese Cederquvist and Mr. Andi Junirsah are highly acknowledged for their help in the daily life arrangements. All the staff at Äspö are acknowledged for their friendliness and kind hospitality.